5-2022

Behavior of Narrow Mechanically Stabilized Earth Walls with Secondary Reinforcement

Abraham Alejandro Alvarez Reyna
The University of Texas Rio Grande Valley

BEHAVIOR OF NARROW MECHANICALLY STABILIZED EARTH WALLS WITH SECONDARY REINFORCEMENT

A Thesis

by

ABRAHAM ALEJANDRO ALVAREZ REYNA

Submitted in Partial Fulfillment of the

Requirements for the Degree of

MASTER OF SCIENCE

Major Subject: Civil Engineering

The University of Texas Rio Grande Valley

May 2022

BEHAVIOR OF NARROW MECHANICALLY STABILIZED EARTH WALLS WITH SECONDARY REINFORCEMENT

A Thesis
by
ABRAHAM ALEJANDRO ALVAREZ REYNA

COMMITTEE MEMBERS

Dr. Thang Pham
Chair of Committee

Dr. Thuy Vu
Committee Member

Dr. Mohamed Abdel Raheem
Committee Member

Dr. Jong Min Kim
Committee Member

May 2022

ABSTRACT

Alvarez Reyna, Abraham A., Behavior of Narrow Mechanically Stabilized Earth Walls with Secondary Reinforcement. Master of Science (MS), May, 2022, 74 pp., 9 tables, 26 figures, references, 43 titles.

Mechanically Stabilized Earth (MSE) walls have been used in past decades as an alternative, cost-effective, and performance solution to replace conventional retaining walls. AASHTO guidelines recommend a reinforcement length-to-height ratio of 0.7. However, this ratio is not applicable where there exist constraint conditions. FHWA guidelines recommend the minimum reinforcement length-to-height ratio of 0.3 for Narrow Mechanically Stabilized Earth (NMSE) walls in these cases. However, published guidelines have not sufficiently accounted for several parameters influencing NMSE performance and efficiency. Using finite element analysis (PLAXIS 2D), this study focuses on finding a relation between the length-to-height ratio and other parameters/components of the NMSE walls that influence the behavior and structure of NMSE walls. Moreover, length-to-height ratios from 0.3 to 0.5 were targeted, and effects of secondary reinforcement layers were applied. With a proposed reinforcement configuration, the lateral displacement can be reduced significantly and the amount of reinforcement material to be used.

DEDICATION

This thesis is dedicated to my dear and loving parents, Pastor/Engineer Oscar Arturo Alvarez Rios and Doctor/Theologist Nancy Maria Reyna Aguilar who have formed the person I am today with constant loved, wisdom and care. I am eternally grateful with God for all the opportunities and blessings I was able to experience throughout my life and educational goals.

ACKNOWLEDGMENTS

I would like to express my sincere gratitude to my thesis advisor, Dr. Thang Pham for his continuous support and knowledge sharing on the subject of study. Every valuable lesson impacted positively my way of thinking in engineering. I also wish to thank the thesis committee members Dr. Thuy Vu, Dr. Mohamed Abdel Raheem, and Dr. Jong Min Kim who follow and care for my educational growth since my bachelor's degree.

A special thank-you is extended to Dr. Thuy Vu for her decision of introducing me to the civil engineering research area creating a great impact on my educational and life decisions.

Moreover, I would like to express my gratitude to my previous mentors and supervisors Maria Del Carmen Gomez Navarro, Guadalupe Vargas, and Angela Peña. Their strong commitment and guidance during my professional career, assist me to mature in the labor sector and true friendship that I will always appreciate.

Finally, I truly appreciate my brothers Oscar Arturo Alvarez Reyna and Ricardo Angel Alvarez Reyna for encouraging me to follow my dreams and helping me in several ways.

TABLE OF CONTENTS

Page

ABSTRACT iii
DEDICATION iv
ACKNOWLEDGMENTS v
TABLE OF CONTENTS vi
LIST OF TABLES viii
LIST OF FIGURES ix
CHAPTER I. INTRODUCTION 1
CHAPTER II. LITERATURE REVIEW 4
2.1 Geosynthetic Reinforced Soil Mechanism 4
2.2 Centrifuge Modeling of Shored MSE Wall 8
2.3 Field-Scale Testing of NMSE Wall 11
2.4 Numerical Methods 18
2.5 Arching Effect 22
2.6 Secondary Reinforcements 26
CHAPTER III. METHODOLOGY 31
3.1 PLAXIS2D 31
3.2 Model Properties 33
3.3 FEM Model Steps 37
CHAPTER IV. RESULTS AND DISCUSSION 42
4.1 MSE and NMSE Modeling 43
4.2 Secondary Reinforcement Configuration 46
4.3 Test 1: Traffic Load Analysis 53
4.4 Test 2 Secondary Reinforcement Comparison Test 56
4.5 Test 3: Length to Height Ratio Test 58
4.6 Test 4: Reinforcement Length Comparison 60

4.7 Test 5: Geosynthetic Material Use Test 62
4.8 Test 6: Reinforcement Tensile Strength Test 64
CHAPTER V. CONCLUSIONS 66
REFERENCES 68
APPENDIX 72
BIOGRAPHICAL SKETCH 74

LIST OF TABLES

Page

Table 3.1: Properties of backfill soil used for model (Pham, 2009) 34
Table 3.2: Reinforcement Properties (Pham, 2009) 35
Table 3.3: Wall Facing Properties (Pham, 2009) 35
Table 3.4: Interfaces Properties (Pham, 2009) 36
Table 3.5: Interfaces Properties (Huang et al. (2009) 36
Table 4.1: Numerical Model Configuration 47
Table 4.2: Test 4 Reinforcement Length Configuration 48
Table 4.3: Total Number of Tests 48
Table 4.4: Reinforcement Material Comparison 49
Table A.1: State of the Art Equipment 73

LIST OF FIGURES

Page

Figure 2.1: Bearing capacity pressure versus Settlement Curves for 0.46 m footing series by Adams et al. (1997) 7

Figure 2.2: Woodruff (2006) Centrifuge model test set-up 9

Figure 2.3: FHWA-CFL/TD-06-001 Shored Mechanically Stabilized Earth (SMSE) Wall Systems Design Guidelines 9

Figure 2.4: Test wall plan view (FHWA – Turner Fairbanks Highway Research Center (TFHRC) 12

Figure 2.5: Test layouts from the models with reinforcement layers fixed to the stable wall at the rear. (a) connection of four layers (b) connection of upper two layers (Kakrasul., 2018) 15

Figure 2.6: Test layout from models with reinforcement layers bent upward with a different aspect ratio (B/H) 0.3 H wall with footing offset of 0.05m (b) 0.5H wall with footing offset of 0.15m 16

Figure 2.7: Traditional MSE Wall 27

Figure 2.8: Shallow failure mode between layers of primary reinforcement (a) without secondary reinforcement; (b) with secondary reinforcement (Michalowski 2000) 28

Figure 3.1: Geometry generation of an L/H 05. Wall with a reinforcement spacing of 0.2m 38

Figure 3.2: Mesh generation of the L/H 05 with a reinforcement spacing of 0.2m. 38

Figure 3.3: Construction phase of the first layer. 40

Figure 3.4: Deformed mesh of 0.5 L/H Wall with a spacing of 0.2m at 200kPa Normal Test 41

Figure 4.1: PLAXIS model of Huang et al. (2009) full-scale wall 44

Figure 4.2: Lateral displacement comparison of Huang's wall and PLAXIS model 45

Figure 4.3: Models with primary reinforcement only 50

Figure 4.4: Models with the addition of secondary reinforcement 51

Figure 4.5: Model with an L/H ratio of 0.3 51

Figure 4.6: Models with different reinforcement lengths with an L/H ratio of 0.5 52

Figure 4.7: Traffic load analysis test results. (PR): Primary Reinforcement / (SR): Secondary Reinforcement / (L/H): Length to Height Ratio 54

Figure 4.8 Traffic load analysis test for models 1 through 8. 55

Figure 4.9 Secondary reinforcing spacing test Results. 57

Figure 4.10: Length to height ratio test results 59

Figure 4.11: Reinforcement length test results 61

Figure 4.12: Maximum lateral displacement test results at 200kPa 62

Figure 4.13: Geosynthetic usage comparison 63

Figure 4.14: Reinforcement tensile strength test results 65

CHAPTER I

INTRODUCTION

Mechanically Stabilized Earth (MSE) walls have been used in the past decades as an alternative, cost-effective, and performance solution to replace conventional retaining walls in geotechnical and earthwork engineering projects.(LUO et al., (2014); Yang and Liu (2007; Kniss et al., 2007. MSE walls are typically compacted backfill soil with geosynthetic/steel reinforcements material in layers and a facing wall for aesthetic purposes. According to the Federal Highway Association (FHWA) guidelines, a base-to-heigh ratio of 0.7 is recommended for safety purposes. However, a 0.7 B/H ratio is not applicable in all cases due to the project's nature constraints, such as widening an existing road in a mountainous area. Introduction of Narrow Mechanically Stabilize Earth (NMSE) walls study emerged to solve this case. NMSE walls must achieve equal performance even though lateral displacement is more accessible to take place due to the lack of space, hence preventing failure (Morrison et al., 2006; Kniss et al., 2007; Yang and Liu., 2007),

Narrow Mechanically Stabilized Earth (NMSE) walls retain soil or support pavement/roadway in narrow areas. Consequently, demand for NMSE walls increases in locations where rare natural conditions predominate. The walls must withstand lateral earth pressures exerted from the soil and external loads of other natural sources to prevent failure, but lack of space availability difficulties this task. Recommended reinforcement length-to-height

the ratio of 0.7 is not possible in narrow areas. Besides preliminary reinforcement layers, secondary reinforcement layers are added to increase the wall's local and overall stability and performance.

Several researchers proposed secondary reinforcement as a viable option for assisting in the connection force reduction of MSE walls (Leshchinsky, 2000). Following the current topic of discussion, typical MSE walls with secondary reinforcement layers are rarely investigated, showing a lack of studies on full-scale models, and occasionally, numerical or analytical studies are presented. Furthermore, secondary reinforcement layers on narrow MSE walls have even less focus on investigation, bringing several unknowns on how and what affects the wall performance.

This article will focus on finding a relationship between the L/H ratio and MSE internal stability by adding secondary reinforcement using the finite element analysis software PLAXIS2D. Moreover, the study focuses on finding the parameters influencing the efficiency and performance of an NMSE wall, such as soil and reinforcement properties, vertical reinforcement spacing, and reinforcement length. NMSE models ranging from 0.3 to 0.5 L/H ratio were targeted. For this study, an extensive literature review was conducted on MSE walls, NMSE walls laboratory, field-scale, numerical modeling testing, geosynthetics, soil properties, and Compaction Induced Stresses (CIS) contribution of soil strengthening, and secondary reinforcement in retaining and MSE walls.

The effects of secondary reinforcement layers, added to increase the local and overall stability of the wall and the wall performance, were studied intensively, and an analytical equation for estimating the length of secondary reinforcement layers was proposed. Adequate conditions to add secondary reinforcement layers were introduced to reduce the amount of reinforcement and increase the performance of the NMSE walls; the addition of the secondary reinforcement layers can help reduce local failures and lateral earth pressure acting on the wall facing. Compaction-induced stresses on NMSE walls during and after wall construction were also investigated.

CHAPTER II

LITERATURE REVIEW

A GRS mass is a soil improvement technology composed of horizontal geosynthetic on a soil body. Several testing methods have been used to analyze the behavior of geosynthetics concerning soil integrity and performance under different conditions. This chapter focuses on the previous studies regarding the soil mechanism with reinforcement interaction, the various methods used, and the addition of secondary reinforcement layers.

2.1 Geosynthetic Reinforced Soil Mechanism

The study of geosynthetics primarily focuses on soil improvement when reinforcement is added to a soil body. Popular concepts explaining this behavior were developed by Scholsser and Long (1972) and Yang (1972) with the apparent cohesion theory and increasing apparent confining pressure theory (as cited in Pham, 2009). The first concept explains a significant major principal stress increase when a triaxial test sample is reinforced; this is visualized by comparing Mohr circles generated at reinforced and unreinforced sample material layers, where cohesion is present in the first-mentioned. The second concept shows an axial strength and confining pressure increase at the reinforced soil triaxial test result. (Pham, 2009). Following these two concepts, an equation is formulated using Rankine's earth pressure theory, where apparent

cohesion and friction angle can be determined as a function of strength and spacing. Nonetheless, Pham (2009) conveys the questionability of this equation since it assumes that apparent cohesion is the result of the strength value times the passive lateral earth pressure, all divided by the spacing value. It implies an increase in strength with decreasing spacing.

Furthermore, studies regarding soil improvement were followed by Professor Bengt Broms by inserting geosynthetics in a triaxial test. Broms (1977) proved how the location of the reinforced material induces a significant effect on stiffness performance. Four scenarios were tested in which the area influences the soil strength results. The first scenario deals with a no-reinforcement test, followed by a reinforcement near the top and bottom test. Furthermore, the third test follows the same conditions as the previous model, including an extra middle layer. The fourth trial has four evenly distributed reinforcement layers at the sample height. The No-reinforcement test and reinforcement near the boundaries test were the same in terms of stress-strain curves as given by the results.

In contrast, the third and fourth trials acquired considerable performance values. This study suggests that proper spacing placement in a GRS structure will improve the performance and efficiency of the wall. Therefore, this study will also aim to include spacing at the most favorable location. As previously mentioned, Broms' study was conducted in a typical small triaxial test, while the modeling of this paper will focus on actual GRS structure on a large scale. Applicability may not be as accurate as in a real case scenario but assist in denoting the reinforcement's behavior.

Moreover, GRS mechanics research is performed with laboratory analysis or numerical modeling methods used to explain the behavior of soil body interaction with geosynthetics. Numerical models typically used are the Discrete Element Method (DEM) or Finite Element

Method (FEM). An example of combining both concepts is shown by Ling et al. (2000) in the GRS-Finite Element Method study with modular block facing. Such investigation also used laboratory and FEM testing analysis of a full-scale GRS wall with secondary reinforcements. Results gave an insight into how the soil body behaved, showing a significant displacement at the middle height of the wall after the construction of the model.

Moreover, the paper explains the importance of adding the compaction process after completing each layer for proper strength behavior. Furthermore, lateral stress distribution improves as the construction process reaches its final stage, and larger values of vertical stresses are located at the front end of the wall. Results were identified by testing predicted (finite element method) and measured (laboratory) results. A comparison is made between wall elevation and displacement concerning the load applied to the test (Ling et al., 2000).

Furthermore, several designers focus on the reinforcement material rather than spacing during construction planning on GRS structures. On the other hand, construction professionals learned by experience that GRS performance is not only contributed to the material's strength (Pham, 2009). According to the spacing and number of reinforcement layers chosen for the project, Adams et al. (1997) conducted a large-scale model load test to confirm a reinforced soil foundation's behavior. The Federal Highway Administration (FHWA) conducted the experimental analysis to further understand the mechanics of a GRS technology. In their research, 34 load tests were conducted to analyze two types of geosynthetics concerning multiple uses of layers in the structure use. The tests consisted of one layer to three layers, and the addition of tests with geocell implemented at a reinforced concrete test pit with the large-scale dimensions of 6.4m (wide) x 6.9m (long) x 6m (deep) Adams et al. (1997). Their results strongly agree with an increase in soil ultimate bearing capacity by using a GRS technology

(Adams et al., 1997). This result is illustrated as the differences in Bearing Capacity Ratio (BCR) achieved by every test with different reinforcements, spacing, and load combinations. BCR is the RSF bearing capacity value divided by the footing without reinforcement bearing capacity (Adams et al., 1997). Thus, the greater the BCR, the better the test's performance can be. Figure 2.1 presents the results for the bearing pressure for settlement of seven tests: one without reinforcement and the other 6 with two types of reinforcements. It is concluded that the geogrid model presents better soil performance comparing no reinforcement and geocell models.

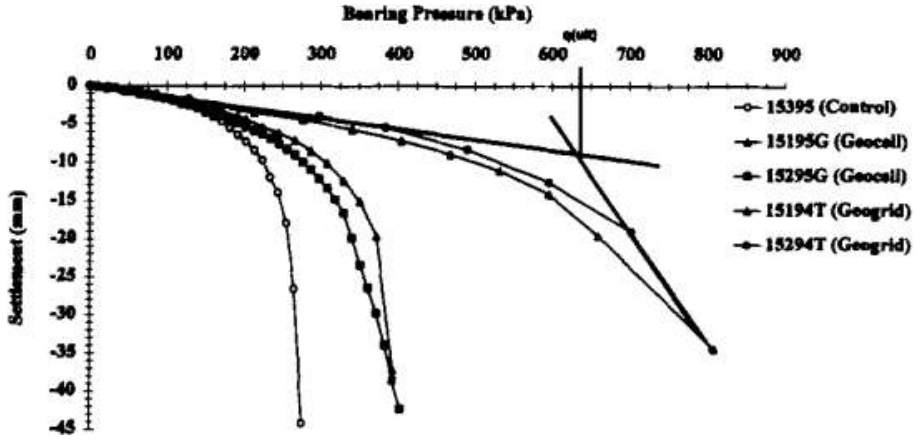

Figure 2.1: Bearing capacity pressure versus Settlement Curves for 0.46 m footing series by Adams et al. (1997)

Moreover, due to the adversity and cost-demanding required for full-scale models, few studies concerning MSE large-size tests in the scientific community are available. From this type of study, several conclusions were withdrawn. Load capacity received a substantial influence from spacing rather than the strength properties of the reinforcement material. (Elton and Patawanran., 2005; Adams., 1997; Ziegler et al., 2008) Adding reinforcement materials with greater strength instead of focusing on the spacing has been a flawed concept utilized for achieving greater performance. Chen et al. (2009) conducted a study focused on investigating the

behavior of spread footings inserting reinforcement layers. Twenty-two tests were made with several scenarios such as no reinforcement, one-layer reinforcement, or three layers tests. This last test agrees with the number of layers used for conducting the tests in Adams et al. (1997). Chen et al. (2009) concluded that reinforcement strength has a more significant effect after testing seven different strength types of reinforcements, one with steel wire mesh and another with steel bar mesh. This conclusion agrees with Broms's (1977) analysis concerning soil layering.

2.2 Centrifuge Modeling of Shored MSE Wall

Centrifuge testing or laboratory-scale modeling is considered an excellent tool to evaluate the Short MSE reinforcements according to the FHWA in 2006. The first centrifugal study related to shored MSE walls was given by Frydman and Keissar (1987), where their testing used different aspect ratio scenarios; the results convey a decrease of earth pressure named the "arching effect" concerning depth. (Kniss et al., 2007) This topic will be covered later in the paper. Moreover, Take and Valsangkar (2001) continued studying narrow MSE walls using the centrifuge model test. Take, and Valsangkar used an aspect ratio from 0.1 to 0.7 compared to Frydman and Keiser, which used a percentage from 0.l1 to 1.1. Their studies also agree with a decrease of lateral earth pressure concerning depth. (Kniss et al., 2007) One significant contribution dealing with several scenarios of narrow MSE walls is given by Woodruff (2003). He conducted a parametric study for aspect ratio, reinforcement strength, spacing, shoring wall inclination, etc. His contribution deals with 24 tests made with the focus on reducing the length of the reinforcement. Using two types of soils and support, tests varied in weak or strong

directions reinforcement, variety of soil, spacing, and different reinforcement lengths. Figure 2.2 shows the centrifuge model test set-up used for the analysis, and figure 2.3 shows the results distributed in 7 test series.

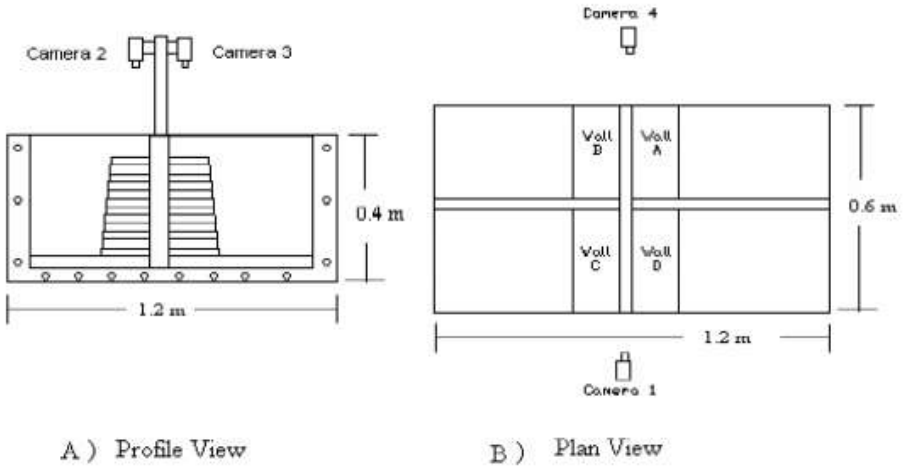

Figure 2.2: Woodruff (2003) Centrifuge model test set-up

Test Designation		Aspect Ratio	g-Level at Failure	Failure Type[1,2]	g-Level at Pull Away
1	a[3] (Control)	0.9*H*	18	Internal [(1)]	N/A
	b	0.6*H*	17	Compound [(1)]	17
2	a	0.6*H*	38	Compound [(1)]	27
	b	0.4*H*	41	Compound [(2)]	39
3	a	0.7*H*	38	Internal [(1)]	N/A
	b	0.7*H*	49	Internal [(1)]	N/A
	c	0.7*H*	47	Internal [(1)]	N/A
	d	0.7*H*	44	Internal [(1)]	N/A
4	a	0.7*H*	N/A	N/A	N/A
	b	0.5*H*	N/A	N/A	N/A
	c	0.3*H*	N/A	N/A	22
	d	0.3*H*	N/A	N/A	32
5	a	0.17*H*	7	Overturning [(2)]	5
	b	0.2*H*	N/A	N/A	N/A
	c	0.25*H*	32	Overturning [(2)]	13
	d	0.2*H*	N/A	N/A	N/A
6	a	0.3*H*	N/A	N/A	27
	b	0.3*H*	N/A	N/A	30
	c	0.2*H*-0.3*H*	78	Overturning	25
	d	0.3*H*	N/A	N/A	N/A
7	a	0.25*H*	38	Overturning [(2)]	31
	b	0.25*H*	2.5	Overturning [(2)]	1
	c	0.25*H*	1	Overlap pullout	N/A
	d	0.25*H*	1	Overlap pullout	N/A

Figure 2.3: FHWA-CFL/TD-06-001 Shored Mechanically Stabilized Earth (SMSE) Wall Systems Design Guidelines.

The first series deals with a 0.6H/B shored wall with a weak perpendicular oriented reinforcement. The second test is an unconnected system with reinforcement lengths of 06 and 0.4 and the same orientation as test 1. Test series 4 included models of 0.3H reinforcement length that were not able to fail, although the pulling away effect occurred near the shoring. Meanwhile, other testing had 0.7 with no pulling effect. Test series have an overturning failure with models of 0.17H as expected for small reinforcement lengths. However, having 0.2H reinforcement lengths with a wrap-around design did not present failure. Test series 6 is the only model that failed to overturn a standard model. The other three models of the test series had attributes that make the models more robust such as top reinforcement tied or wrapped at the back of the support.

Lastly, test series 7 investigated the strong mounts with short reinforcement lengths of 0.25H. Still overturning failure at the 10- and 30-mm spacing models were obtained, and pullout failure at the model of 30 mm (Woodruff., 2003)

Several conclusions are withdrawn from Woodruff experiments regarding aspect ratio, reinforcement strength, shoring interface, reinforcement configuration, vertical spacing, and shoring wall batter. The aspect ratio of the wall will influence the failure type of the MSE wall. It was concluded that aspect ratios larger than 0.6 fail from internal failure, while equal to or less than 0.6H ratio has a compound failure, and a ratio less than 0.3 obtained overturning failure. Strong reinforcement influenced internal failure prevention compared to testing with low tensile strength reinforcement models. Likewise, the study found effectiveness in smooth shoring walls even though it was expected to see improvement in rough shoring walls. Earth pressures reduction is achieved after wrapping around the back of the reinforcement layers and reducing lateral earth pressures with decreasing spacing for short MSE walls.

Moreover, another conclusion withdrawn from this study is that stability is assisted by inclining the shored wall. The failure surface in this test type was bilinear type instead of linear. (Lawson and Yee., (2005); Morrison et al., 2006; Woodruff, 2003; Yang and Liu., 2007; Yang et al., 2011) This result concludes that conventional Rankine's method for location failure surface will be conservative due to the difference in pattern. (Yang et al., 2011) Continuation of Woodruff experiments are presented at the field scale testing, which took the information of the centrifuge modeling.

2.3 Field-Scale Testing of NMSE Wall

Another type of testing used in the study for Narrow MSE walls is Field Scale Testing. This method used more realistic dimensions compared to centrifugal testing. As well as the previous process, several researchers and governmental entities conducted their studies using this method. FHWA is one of the US government entities that conducted field-scale testing to analyze two hypotheses: Shoring walls reduce external lateral loading and small benefit of connected SMSE walls systems compared to unconnected ones.

For the field-scale wall test from FHWA, a model was divided into half connected and half unconnected systems with aspect ratios from 0.25H to 0.39H. The bottom reinforcement length of 1.4 m, reaching 2.14m, the top reinforcement, and two load footings are distributed accordingly to the connected and unconnected sections of the wall. (Morrison et al., 2006) Several measurement instruments were used to detect stress and strain distribution, stress changes, surcharge load increases, etc. Regarding the load program, eight jacks were used, four per footing, to make load increases until reaching 890kN load per footing. Slack was developed at the face of the wall during the program. Strain gages assisted in obtaining the local stress and strain distribution at four points of geogrids in the wall and, at the same time, visualizing the

maximum pressure in both connected and unconnected systems. A strain increase was observed as the measured results increased with the elevation and surcharge load increase. There was a slight difference in both systems agreeing with the hypothesis of minor benefit (Morrison et al., 2006). Figure 2.4 shows the test wall plan view used for this model.

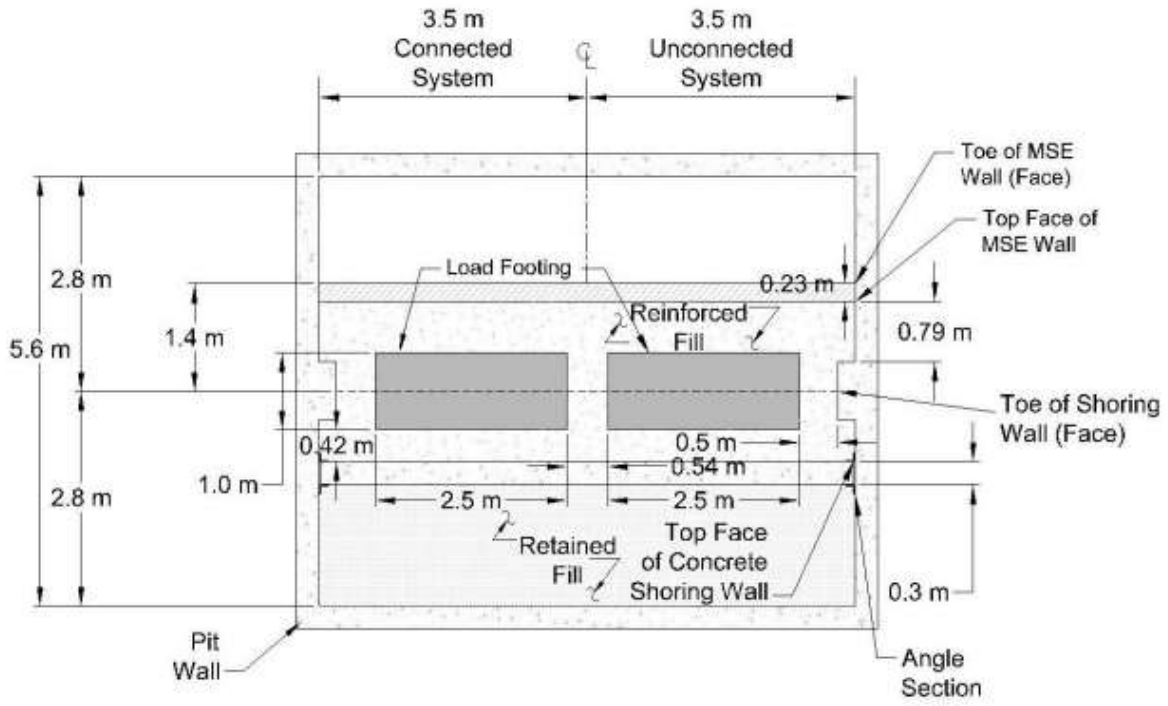

Figure 2.4: Test wall plan view (FHWA – Turner Fairbanks Highway Research Center (TFHRC)

For the lateral earth pressure cells, Rankine active earth pressure (σ_h) was used as:

$$\sigma_h = \gamma H K_a + q K_a \quad (2.1)$$

γ: Unit weight of soil

H: Height of the wall

K_a: Active earth pressure

q : Surcharge loading

The results showed a general increase in lateral earth pressures as surcharge load increased in both cases (connected and unconnected). Higher lateral earth pressure is recorded at the top for the connected wall, while lower values are found for the loose wall. These low readings from the unconnected wall may be attributed to the untied system to the shoring wall, generating tension cracks. Furthermore, the lateral earth pressures for connected and unconnected are less than or equal to Rankine active earth pressures. (Morrison et al., 2006)

For the vertical earth pressures, the indication of arching can be attributed to the small percentage of vertical pressures found at the base of the wall near the shoring wall. This is attributed to the shoring wall assistance by absorbing the vertical pressures. In terms of horizontal displacement, the unconnected model presented greater values than the connected model; the authors recommend adding extensions to the upper part of the wall. Furthermore, Linear Variable Differential Transformer (LVDT) readings show a small settlement in the corresponding wall compared to the unconnected wall for vertical displacement. The connected wall goes from 1 mm at the base to 18 mm at the center for lateral displacements. The unconnected wall readings were not accurate; instead, only one reading gave 11 mm removal at

the top. The results reproduced small geogrid strain data and small vertical and horizontal deformations of MSE walls, comparing connected and unconnected systems. Therefore, similar behavior can be expected from both. Thus, there is no benefit when using one model or other only in limiting the tension crack potential in the unconnected model. Furthermore, the use of Shoring walls with MSE reduces lateral loadings.

Moreover, due to limited information, Kakrasul (2018) conducted a performance evaluation study concerning narrow geosynthetic reinforced retaining walls (GRR Walls). Kakrasul conducted several model tests with varying specific parameters such as changing the aspect ratio from 0.7 to 0.5 or 0.3, connecting the reinforcement to the fixed, stable wall, unconnected, or connected only at the top layers, variation of reinforcing spacing, variation of footing offset from 0.20 m to 005 proximity to the facing wall, and reinforcement layers bent upward. Figures 2.5 and 2.6 show some of the test layouts of the different models analyzed.

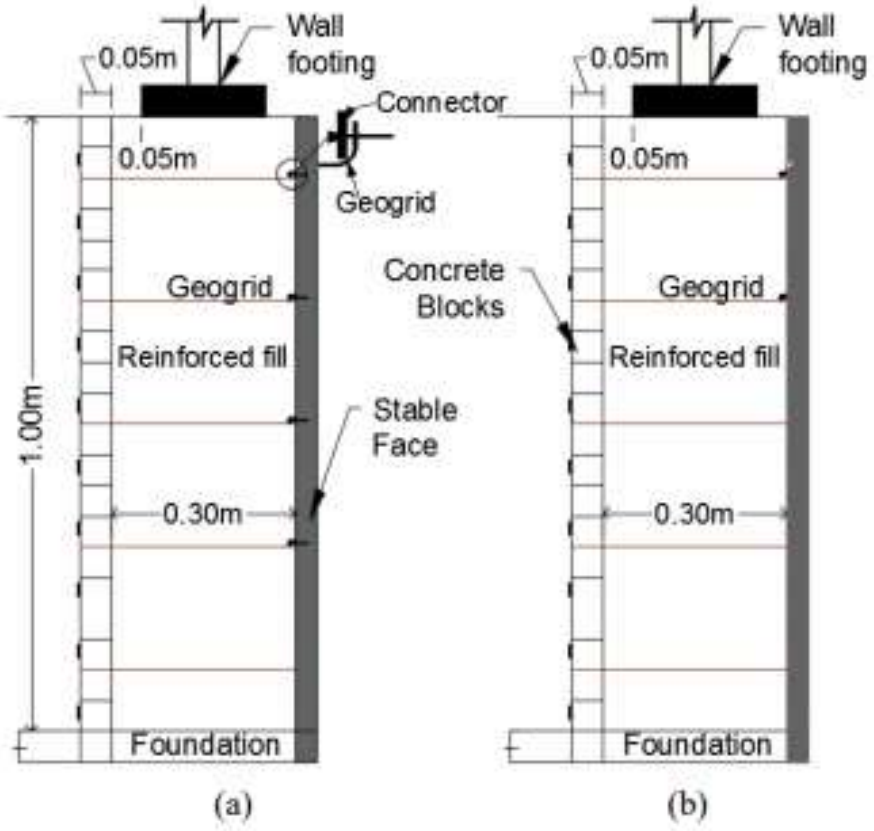

Figure 2.5: Test layouts from the models with reinforcement layers fixed to the stable wall at the rear. (a) connection of four layers (b) connection of upper two layers (Kakrasul., 2018)

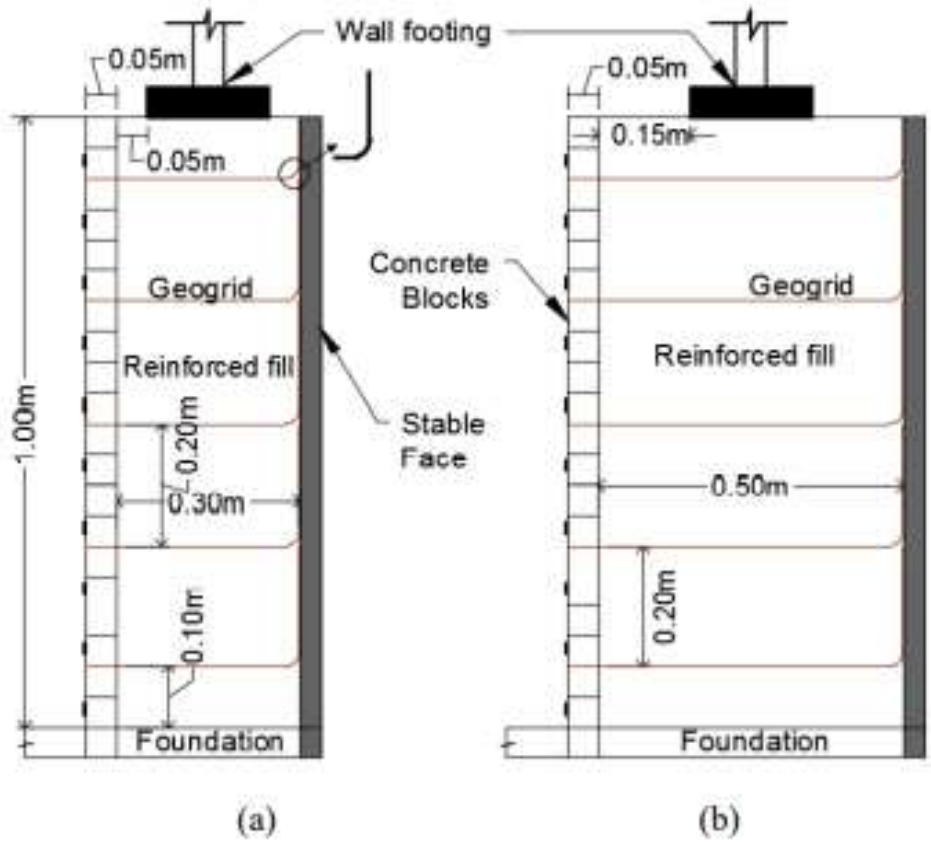

Figure 2.6: Test layout from models with reinforcement layers bent upward with a different aspect ratio (B/H) 0.3 H wall with footing offset of 0.05m (b) 0.5H wall with footing offset of 0.15m (Kakrasul., 2018)

Eleven models were tested under a parametric study regarding wall performance. From the results, several conclusions were given for lateral displacement, settlement of footing, vertical earth pressure, and lateral earth pressure. There is an increase in lateral displacement concerning the applied load from all models.

From the results of 0.7H aspect ratio models with retained fill and with no contained fill, there is a slight difference due to the proximity of the stable wall concerning the reinforced filler. Thus, there is an agreement of difference in stress distributions. Furthermore, comparing models

with reinforcement length difference (from 0.7H to 0.5H) resulted in more significant maximum displacement and reduction of bearing capacity. Comparing 0.7H to 0.3H, there was greater excellent vertical compression, more significant vertical stresses, and deformation as the ratio decreased. (Kakrasul., 2018)

Changing from 0.2 to 0.05 footing offset, an increase in lateral facing displacement is observed due to footing proximity to the facing wall. Thus, higher pressure near the wall can be expected. Comparing connected to the stable wall with nonconnected models, the first one shows a reduction in displacement. Upward bending of reinforcement layer models also gives a reduction of lateral displacement. Compared with the upward bending reinforcement layer model, the connected model presents better effectiveness in terms of lateral displacement reduction (Kakrasul., 2018)

Secondly, no retained fill model presented better ultimate bearing capacity and most minor settlement in footing. Models with 0.7 and 0.5H ratios gave the same settlement results at a specific load applied. However, changing to a 0.3H model shows a more significant settlement with failure as observed. Additionally, greater undersized offset footing reveals a more substantial settlement as well. An increase of bearing capacity is observed in closer spacing models, with connection to the stable wall and with upward bending reinforcement layers and a tendency to settlement reduction. (Kakrasul., 2018)

Thirdly, in terms of vertical earth pressure, the models were expected to increase as there was an increase in the applied load from the footing. The models' analysis was compared to the vertical earth pressure results using the 2:1 method. The previous results compared the results using Rankine theory and Janssen's arching theory for lateral earth pressures. Regardless of the system used, they mostly agree with the pattern of the results most of the time. As well as

vertical earth pressure, there was an increase in lateral earth pressure with the rise of footing load. The footing offset near the facing wall model recorded a higher lateral earth pressure. This is due to the distribution of the applied load in the narrow area. At the 0.3H model, the lateral earth pressure did not behave as expected. Thus, the forces did not follow Rankine's active condition.

2.4 Numerical Methods

FEM and DEM methods are excellent tools used to research soil reinforcement projects. The use of one program type for the other depends on the user's criteria. Vulova and Leshcinsky's (2003) study used FLAC3D, a FEM program to investigate the spacing influence and reinforcement length by using minimal aspect ratios such as 0.17 and 0.19 with reinforcement spacings of 0.2 m and 0.4 m, respectively. The first case failed by overturning, while the second failed the compound. Compound refers to both points of either sliding or overturning. Another observation made in both cases is that stresses were more prominent near the face than at the end of the fill. This is understandable since the width of the fillings was very small compared to the height of the entire MSE and agreed with Kakrasul (2018) and Morrison et al., 2006. Their results indicated that the lateral earth pressure coefficient decreases, and the aspect ratio decreases.

Furthermore, one of the first finite element method (FEM) analyses conducted for understating certain factors of the MSE wall was given by Collin (Morrison et al., 2006). His findings proved the importance of reinforcement strength and pullout for the internal stability of the wall.

Moreover, Budge et al. (2006) calibrated a finite element model of an MSE wall using the PLAXIS program. The main focus of this study was to analyze the vertical displacement of the model in terms of settlement and calibrate the model with an MSE project located in Salt Lake, Utah. Furthermore, the concept of Hardening soil is introduced in this article to improve the soil behavior model. Mohr-Coulomb model is widely used as a simple linear elastic perfectly plastic model that allows representing soil behavior linearly in stress and strain. However, this behavior is not true when the soil is subjected to changes in stress or strain. For this reason, Hardening Soil Model is used to model a not fixed principal stress space, where the model can expand due to plastic straining (PLAXIS., 2020). From Budge et al. (2006) study, a good agreement with the calibration of the model is achieved for settlement concerning depth.

Kniss et al. (2007) studied earth pressures produced at narrow MSE walls in front of a stable slope. The study focused on comparing the expected experimental earth pressures and arching equation with a finite element method model and the study of the aspect ratio effect for earth pressures at rest conditions. Kniss used Frydman's centrifuge test (Frydman et al., 1987) and Take's centrifuge test (Take et al., 2001) to verify the numerical model made with the program PLAXIS. Regarding the earth pressure predictions, good agreement was achieved with the finite element method model to reduce eath pressure with depth and arching effect. Results for the wall aspect ratio of 0.7 also show good agreement for inextensible, stiff reinforcement.

Yang and Liu (2007) conducted a finite element analysis on narrow retaining wall earth pressures at rest and active conditions. From the article, emphasis is given to the aspect ratio playing a significant role in earth pressures distribution. The verification comes from Jacky's passive earth pressure coefficient formula, and Rankine's theory for active earth pressure does not adequately model the narrow MSE wall's behavior. Furthermore, Yang and Liu illustrated the

importance of the arching effect presented in Jaret et al. (1995) to describe the arching impact on these types of walls. Yang et al. (2008) continued by studying the MSE wall using numerical modeling of a centrifuge wall as Kniss et al. (2007) performed. The numerical model had good agreement with the centrifuge test data showing a zero-pressure zone located at the interface between the stable wall and the soil body. Hence, tending to settle in the interface location.

Moreover, Yang et al. (2008)[2] continued with the study sponsored by the Texas Department of Transportation TxDOT for proposing design considerations for Narrow MSE wall systems. Once more, a series of numerical models were conducted by applying limit equilibrium methods, and parametric studies followed the study. Thus, finding the failure surface location and a better understanding of the external failure induced by the MSE wall mechanism is given.

Mahmood (2009) conducted a study of MSE wall failure analysis located in Maryland, Rockville, as part of fulfillment for his thesis. The study involves using PLAXIS to determine the pattern, cause, and mode of failure presented in the real wall. Furthermore, a parametric study is conducted to generate charts that enable the effect of parameters' influence on the wall displacement. From the analysis, the factors identified for failure induced of the wall were the geogrid improper installation, insufficient geogrid length at the upper portion of the wall and the bottom part, and soil low permeability property of the backfill allowing inadequate drainage.

Furthermore, the parametric study also gave an insight into common failure causes of the MSE wall, such as the proper grid length, increase in cohesion value for the soil, and increase in grid strength. Additionally, an analytical model is determined for the required tensile strength of the reinforcement, spacing prescribed value, apparent cohesion, and prediction of lateral displacement. Compaction-induced stresses (CIS) played a significant role in the investigation

since it simulates the soil strength increase during the compaction of the backfill soil layering process.

Following the numerical simulation study, Pham (2009) investigated the composite behavior of GRS mass with different reinforced configurations. A series of large-size Generic Soil-Geosynthetic Composite (GSGC) tests were conducted, and PLAXIS was used to verify the results. Furthermore, the relationship between spacing and strength of the reinforcement is examined, and an analytical model for Compaction Induced Stresses (CIS) evaluation and lateral movement prediction is presented. From the study, several conclusions are withdrawn. The GSGC results appear to be reliable, and the behavior of the GRS mass is observed to be related to spacing and reinforcement strength. A spacing and reinforcement strength equation is developed and verified for use. Furthermore, lateral deformation and compaction operation analytical models are also formulated. From the numerical modeling, reinforcement spacing has a more significant performance effect than reinforcement strength.

Kakrasul (2018) conducted a numerical modeling test using FLAC2D Version 8.0, where the material properties of the reinforced fill, geosynthetic reinforcement, and facing units are given. Compared to the experimental trials, facing displacement was encountered with footing load increase as expected. Same matched results were obtained with the experimental results' lateral displacements and settlement computed. Specific scenarios have a slight deviation in results compared to the experimental type; this is the case for testing a 0.3H wall. The lateral wall facing displacement trend at an applied pressure of 55 kPa is slightly more significant than the experimental result.

2.5 Arching Effect

When an aspect ratio of 0.3H is used, an unexpected decrease in lateral earth pressure appears compared to the lateral earth pressure using conventional guidelines methods. This is attributed to a unique phenomenon at narrow retaining walls denominated as soil arching effect. According to Terzaghi (1943), forces transfer between the mobilized and static parts of the soil due to shear resistance in the interface. Terzaghi (1943) depicts it as a phenomenon that occurs when stress distribution is not equal to the unit weight of the soil according to the depth.

Thus, arching is defined as a re-distribution of stresses due to a lack of movement on the sides. (Han et al., 2016; Han et al., 2017) This is reflected in narrow walls as the space is reduced compared to regular MSE walls. (Han et al., 2016) studied the effect of fully and partially mobilized soil arching effects. Due to the nature of this phenomenon, load distribution and stability may differ in the design of a project. Hence the importance of analyzing this phenomenon. The positive soil arching effect is discovered and defined by the movement of the mobilized portion weight to the sides as the mobilized portion goes down and creates upward shear stress. (Han et al., 2016)

Terzaghi created an analytical method to calculate the re-distribution of loads by applying a trap door test. A vertical stress equation is constructed by observing a curvature pattern in the mobilized portion concerning depth. Assuming the vertical mobilized portion, the equation of vertical stress is defined as:

$$\sigma_v = \frac{B\left(\gamma - \frac{2c}{B}\right)}{2ktan\emptyset}\left(1 - e^{-2ktan\emptyset\frac{z}{B}}\right) + q * e^{-2ktan\emptyset\frac{z}{B}} \quad (2.1)$$

Were:

σ_v = Vertical stress at the bottom of the mobilized portion

B = width if the mobilized portion

c = cohesion of soil

Ø = Friction angle

z = height of the mobilized portion

K = lateral earth pressure coefficient

q = surcharge n the surface

Y = unit weight of the soil

(Han et al., 2016)

In terms of soil arching, Shukla and Sivakugan (2013) developed an extensive analytical method to get Cd as one of the components of the soil arching equation presented by Terzaghi and other authors conducting testing on ditch conduits and how to transfer load from the top part of the conduit to the lateral walls of the ditch.

After the analysis was completed, results showed a load coefficient dependency on several parameters such as coefficient of lateral earth pressure (K), friction cohesion for the granular soil backfill-ditch wall interface (μ), geosynthetic stiffness (E*), nondimensional depth

at the top of the ditch conduit below the ground level (H*), nondimensional depth of the geosynthetic layer above the top of the conduit (h*), and the ruth depth (r*). Previous cases are given where the load coefficient may contribute to changes in the overburden soil weight. A rut depth of 0 implies no deflection, which means there will be no reduction in the overburden soil weight. "Shukla, and Sivakugan (2013)". Another case is when soil arching does not appear if the friction/shear resistance is neglected. This concludes that geosynthetic height above the conduit will not influence the overburden load. As rut depth increases, the load coefficient decreases; this condition can be applied as the geosynthetic stiffness increases or makes the rut depth larger. "Shukla, and Sivakugan (2013)"

Moreover, Kakrasul (2018) mentions other soil arching methods developed as the Janssen equation in a similar study of corn retention in a silo. In other words, a similar scenario of retaining fill in a narrower MSE wall concept. The theory relation to narrow MSE walls comes from the explanation of soil settlement while adding individual soil layers, then creating a vertical shear force due to the friction against the settlement. This force is the one responsible for reducing the lateral earth pressure. Janssen's equation is shown below:

$$\sigma = \frac{\gamma B}{2tan\delta}(1 - e^{-2k\frac{Z}{B}tan\delta}) \quad (2.2)$$

Where:

γ = unit weight of backfill soil

B = wall width

Z = depth from the top of the wall

H = wall height

$\delta =$ friction angle between backfill soil and wall and between backfill soil and stable retained medium

K = lateral earth pressure coefficient.

Kakrasul (2018)

According to several data given by researchers, it must be mentioned that lateral earth pressures using Jensen's method are lower than the Rankine method. Furthermore, Kakrasul (2018) and Yang and Liu (2007) used Janssen's arching theory to calculate the coefficient of lateral earth pressure, and given as:

$$k = \frac{B}{2ztan\delta}(1 - e^{-2k\frac{Z}{B}tan\delta}) \quad (2.3)$$

With the equation, lateral earth pressure of Narrow MSE can be solved instead of using Rankine's theory. This method will be used in this study to compare with other scenarios and further examine the arching effect inshore MSE walls.

2.6 Secondary Reinforcements

Traditional Mechanically Stabilized Earth (MSE) walls use primary reinforcement to prevent global collapse of the structure (Michalowski., 2000). Figure 2.7 shows a typical MSE wall configuration composed of compacted backfill soil with geosynthetic reinforcement and a facing wall. In cases where the performance of the wall is compromised, several suggestions are given, such as adding secondary reinforcement. MSE walls with secondary reinforcement layers are rarely investigated, showing a lack of studies about full-scale models, and occasionally, numerical or analytical studies are present. Thielen and Collin (1993) studied implementing secondary reinforcement to stabilize surficial slopes. This study gives a detailed analysis of this application. Christopher (1997) emphasizes the assistance of secondary reinforcements for compaction improvement, slope stabilization, and sloughing prevention during surface water runoff control evaluation. Several authors remark how the design of slopes with secondary reinforcements does not consider stability analysis. (Koerner., (1997); Michalowski., (2000))

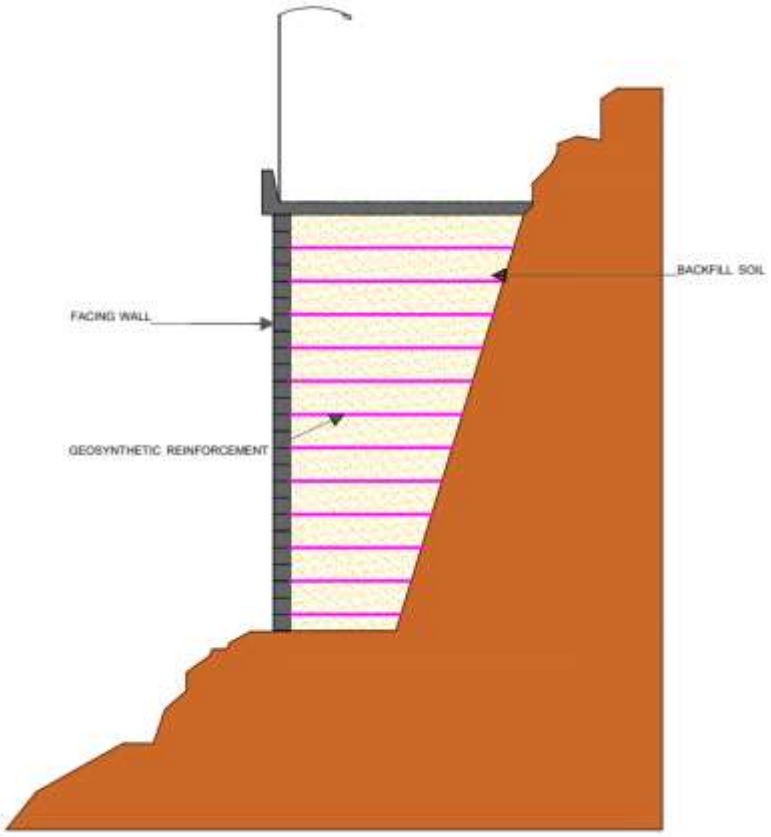

Figure 2.7: Traditional MSE Wall

Michalowski (2000) performed a stability analysis on shallow failures by using limit analysis to find the spacing, strength, and length required for secondary reinforcements. Additionally, a collapse analysis of the soil between the reinforcement layers is also applied to find the cohesion necessary for stability. The method used assists in finding the spacing of secondary reinforcements since cohesion will depend on the size of the mechanism. For better visualization, Michalowski (2000) includes a figure for shallow failure between the primary reinforcement with secondary reinforcement and with no secondary reinforcement, as shown in figure 2.8

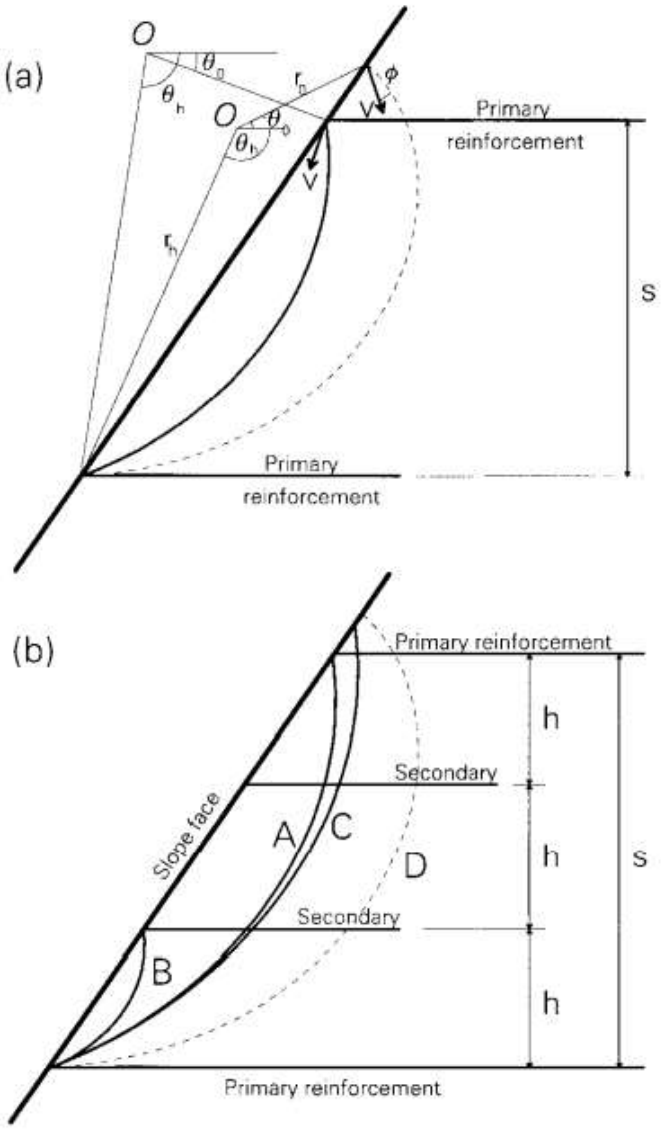

Figure 2.8: Shallow failure mode between layers of primary reinforcement (a) without secondary reinforcement; (b) with secondary reinforcement (Michalowski 2000)

From the study, cohesion will be required if the slope inclination angle of the wall exceeds the internal friction. Secondary reinforcement assists in wall stability by reducing the height of the failure mechanisms of only soil and resistance to the shallow failures. Moreover, an

example is given for calculating the required strength required for primary and secondary reinforcements, proving that minor strength is needed for additional reinforcement. Cohesion necessary to avoid collapse, the needed strength, and the length of the secondary reinforcement is presented in graphical form with the cases of having an MSE wall inclination angle slope between 20 to 60 degrees. At the same time, the method counts for slope and embankments reinforced with geogrids and does not apply to wrapped around facing walls. Leshchinsky (2000) recommended the inclusion of secondary reinforcement layers in case of having a large vertical spacing between the primary reinforcements. Leshchinsky justifications are the increase of internal stability, compaction improvement near the wall facing, and the decrease of primary reinforcement connection loads.

Moreover, Leshchinsky and C. Vulova (2001) used the discrete element program FLAC to investigate the effect of secondary reinforcements on MSE walls performance. From their results, adding secondary reinforcements to the wall could lower the primary reinforcement connection loads, improve internal stability, and shift from connection failure to compound failure. Leshchinsky et al., 2014 introduced a limit state design to investigate the effects of several parameters concerning MSE walls behaviors, including secondary reinforcements. They showed a reduction in connection loads by including the secondary reinforcements.

To this point, theoretical analyses and numerical methods have been employed to investigate the MSE wall's behavior concerning secondary reinforcements. Still, no field test data has been used to verify the assumptions. Jiang et al., 2015 performed a study of three MSE wall test sections. One test section considered uniaxial geogrids for primary and secondary reinforcement, the second test section with uniaxial geogrid for primary reinforcement, biaxial geogrid for secondary reinforcement, and the last test section with primary reinforcements only.

The reinforcement length to wall height ratio (L/H) was approximately 1.6 compared to the 0.7 recommended for the minimum ratio for MSE walls from the FHWA guidelines. Lateral and vertical earth pressures, wall-facing displacement, and geogrids global strains were measured, monitored, and analyzed from these wall sections for 11 months. From the results, vertical earth pressure increased as the wall was constructed. A maximum lateral displacement was also observed at the top of the wall. The two sections containing secondary reinforcements showed less displacement than the test section without secondary reinforcement. For lateral earth pressures at the test wall, sections with secondary reinforcement got a uniform pattern concerning the depth of the wall.

In contrast, the test wall section without reinforcement shows a linear increase pattern with depth. For the coefficient of lateral earth pressure, the two test wall sections with secondary reinforcement were more significant than the test wall section without reinforcement. Small strain values were given for the geogrid connections, and secondary reinforcements took part in the primary reinforcement's tension force.

CHAPTER III

METHODOLOGY

This chapter briefly introduces the finite element program PLAXIS 2D, featuring the major soil modeling components used, followed by the mechanical properties required. Moreover, the modeling sequence steps are explained in detail for the application of PLAXIS. The addition of the secondary reinforcement layers, wall L/H ratio adjustment, reinforcement spacing, and reinforcement strength are investigated.

3.1 PLAXIS 2D

Several finite element programs are available to analyze geotechnical engineering models, such as FLAC, Abacus, Sage Crisp, Sigma, or PLAXIS (Pham, 2009). Chapter II mentions several authors who have successfully used these available programs to simulate soil behavior under interaction with reinforcement materials. The authors that can be mentioned are Yang and Liu (2007), Kniss et al. (2007), Pham (2009), Hossain et al. (2012), Hedge and Roy (2018), and Krakasul (2018), who aimed to simulate MSE and NMSE behavior using numerical methods. Thus, this study selects the software PLAXIS 2D to analyze NMSE walls with secondary reinforcement due to the familiarity with the program. Parametric studies were conducted on factors such as the Length to Height Ratio (L/H), type of reinforcement, spacing influence, facing type, soil type, interfaces between the materials, etc. For this study, PLAXIS

2D is used to create several NMSE wall models with and without the assistance of secondary reinforcement. PLAXIS 2D is a finite element computer program widely used to perform deformation, stress, stability analysis, and water flow behavior modeling in geotechnical and earthwork engineering. The program is divided into five main sections (materials, structures, mesh generation, initial conditions, and construction phase) where the user must follow the order to calculate a complete numerical analysis. Furthermore, the program's first section counts several models to represent the material's behavior, such as Mohr-Coulomb, Soil Hardening, Linear Elastic, Hardening Soil, etc. (PLAXIS, 2020). Due to the facility, researchers' most widely used method is the Mohr-Coulomb model, defined as an elastic, perfectly plastic model. On the other hand, the Hardening Soil model is an advanced elastoplastic constitutive model capable to simulates stiff and soil behaviors by creating an extension of the Duncan and Chang (1970) hyperbolic model. This HSM accounts for the stiffness changes developed during soil compaction, making it stronger. Compared to the Mohr-Coulomb model, HSM can simulate nonlinear behavior, as expected in soil materials. Even though the Mohr-Coulomb model is a good choice for representing soil behavior, the Hardening soil model is selected in this study to explain the soil behavior and to prevent deviations in the actual results.

Section two of PLAXIS offers several tools to simulate structures that will contact the soil to be tested. The available tools are plates, geogrids, soil polygons, displacement or load lines, initial boundary condition interfaces, displacements or load points, tunnel interfaces, anchors, etc. Furthermore, the model's geometry is also created in this section. Section three covers the mesh generation where the meshing distribution method can be specified (coarse, medium, fine). The meshing distribution depends on the model and the user's criteria. As an

illustration, if the user decides to refine the model mesh, a longer computation time will take, but greater accuracy would be expected.

The fourth section covers the model's initial conditions, where initial stresses or initial water conditions are adjusted. For the models tested in this study, no initial conditions were required. Lastly, the construction phase section assists the user in generating multiple phases according to a chronological construction order expected in a real scenario. Huang et al.'s (2009) properties were used to model a wall example in this study, and Pham's (2009) materials properties and interfaces for this study's main NMSE wall models.

3.2 Model Properties

The following sub-section covers the properties required to simulate the models. The MSE wall configuration required compacted backfill soil with reinforcement material and a block-facing wall in case of using Modular Block Facing. Interfaces between the blocks, soil to blocks, and soil to reinforcement were considered. The Hardening Soil Model is used as a better approach to calibrate the study models. HSM stiffness parameters to be used are CD triaxial compression test/plastic strain due to primary deviatoric loading (E_{50}^{ref}), tangent stiffness for primary oedometer loading test/plastic straining due to compression (E_{oed}^{ref}), unloading/reloading stiffness (E_{ur}^{ref}) and a stress-dependent stiffness value according to a power law (m). For the strength parameters, the effective cohesion (C), the effective angle of internal friction (φ), and the dilatancy angle (Ψ) are required (Nasasira Derrick, 2020). Table 3.1 shows the properties used for the soil backfill of Pham (2009) for the main models and Huang et al. (2009) properties for the example model. To manually find E_{50}^{ref} of a soil sample, the assistance of a triaxial stress and strain curve in a combination of equation 3.1 can be used.

Table 3.1 Properties of backfill soil used for model (Pham, 2009)

Parameters	Pham (2009)	Huang et al. (2009)
γ_d (kN/m^3)	24	16.8
γ_w (kN/m^3)	25	-
E_{50}^{ref} (kPa)	63,400	50,000
E_{ur}^{ref} (kPa)	126,800	150,000
m	0.5	0.5
ν	0.2	0.3
φ (°)	50	44
ψ (°)	17	11
c' (kPa)	70	5

$$E_{50}^{ref} = E_{50}\sqrt{\frac{p_{ref}+a}{\sigma_x^{'}+a}} \qquad 3.1$$

Where:

E_{50}^{ref}: Secant stiffness in standard drained triaxial test

E_{50} = Shear hardening secant modulus

p_{ref} = Reference confining pressure (100kPa)

$\sigma_x^{'}$ = Normal stress

$a = ccot(\varphi)$

Schanz (2019) estimated $E_{50}^{ref} \approx E_{oed}^{ref}$ for sands as a shortcut to determine E_{oed}^{ref}.

Moreover, an alternative for getting E_{ur}^{ref} is the relation of $E_{ur}^{ref} \approx 3E_{oed}^{ref}$ given in the PLAXIS Materials-Models Manual as an approximation approach. Table 3.2 shows the geosynthetic properties required to simulate a geogrid component in the project materials section. The material type used for the geosynthetic has elastoplastic characteristics, as recommended by Krakasul (2018). Secant stiffness was utilized for the axial stiffness (EA) and yield strength ($N_{p,1}$) for stiffness as required for the materials menu on PLAXIS 2D. Table 3.3 shows the properties needed to simulate the facing as a linear elastic model. In this case, the wall facing is simulated by individual blocks enabling interfaces between the blocks and the soil. Moreover, table 3.4 deals with the interface properties used in this study's models, while table 3.5 shows the interface properties for the Huang et al. (2009) example.

Table 3.2 Reinforcement Properties (Pham, 2009)

Parameter	Pham (2009)	Huang et al. (2009)
Axial stiffness, EA (kN/m)	1,000	
Ultimate Strength, T_{ult} (kN/m)	70	14

Table 3.3 Wall Facing Properties (Pham, 2009)

Parameter	Pham (2009)	Huang et al. (2009)
FE Model	Linear Elastic Model	Linear Elastic Model
γ (kN/ m^3)	17 (hollow blocks)	
E (kPa)	$3*10^7$	
ν (Poisson's ratio)	0.2	

Table 3.4 Interfaces Properties (Pham, 2009)

Parameter	Reinforcement-Soil	Block-Block	Soil-Block
FE Model	Mohr-Coulomb	Mohr-Coulomb	Mohr-Coulomb
Friction angle ϕ (°)	50	33	35
Dilation angle ψ (°)	0	0	0
Cohesion c (kPa)	70	2	49
Elastic Modulus E (kPa)	$63.40*10^3$	$3*10^6$	$4.44*10^4$
Void Ratio v	0	0.45	0

Table 3.5 Interfaces Properties (Huang et al. (2009)

Parameter	Reinforcement-Soil	Block-Block	Soil-Block
FE Model	Mohr-Coulomb	Mohr-Coulomb	Mohr-Coulomb
Friction angle ϕ (°)	44	25	44
Dilation angle ψ (°)	-	-	11
Cohesion c (kPa)	0	0.1	50
E (kPa)	$1{,}000*10^3$	$1{,}000*10^3$	$100*10^3$
v	-	-	-

3.3 FEM Model Steps

For this study, a length-to-height ratio of 0.5 and 0.3 is used for the main models under different surcharge loads applied; on the other hand, Huag et al. (2009) wall is defined as a 3.6m wall height with retained sand backfill of 6m from the wall's face. The steps used for both cases following the structure of the program are presented below:

1. At the soil module, properties are inserted for the soil, geosynthetic, blocks, and interfaces, following tables 3.1 through 3.5. The materials table of contents has a separate option for defining the materials according to their classification (soil & interfaces, plates, geogrid, plates, and anchors)
2. Once the material's properties are set up, the user can create the geometry model in the structures section using the available soil polygon or individual borehole creation. For purposes of the model, the soil polygon feature best fits the configuration of the walls. The soil body, blocks, geosynthetic layers, surcharge loads, and interfaces are implemented. The soil polygon feature defines the soil body of the study with the dimensions of large-scale testing (L/H of 5 or 3). Figure 3.1 shows the model with the application of materials. In case of not including the respective material information in the geometry of the material, the program will not allow the user to continue with the meshing generation.

Moreover, this area counts with grid generation expanding or minimizing the units per point generated.

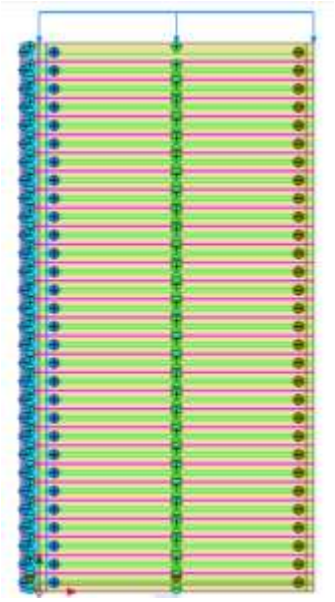

Figure 3.1: Geometry generation of a L/H 05. Wall with a reinforcement spacing of 0.2m.

3. Mesh generation is activated with a medium element distribution.

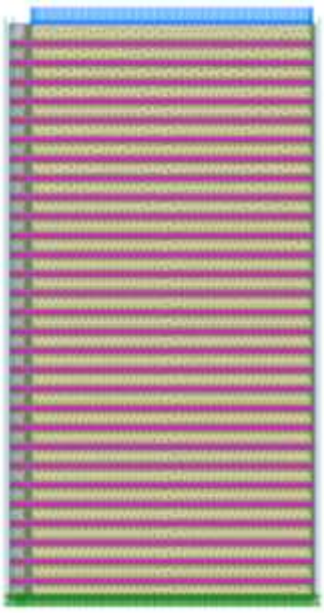

Figure 3.2: Mesh generation of the L/H 05 with a reinforcement spacing of 0.2m.

4. Flow conditions: The water level is not required to adjust since the sample is assumed to be dry. For applying a saturated unit weight of the backfill soil, a value equal to or greater than the dry unit weight can be used to avoid an error message from the program.
5. The construction phase: Before proceeding with the activation of materials or interfaces, the boundary conditions of the phases need to be adjusted as well at the initial phase (0). The x-min boundary condition will cover the vertical wall beginning at point 0 from the x-axis. Since this model has the facing wall orientation from the left, and to avoid displacement during the construction process, the boundary condition is applied as horizontally fixed, allowing displacement on the y-axis but limiting displacement on the x-axis. X-max boundary condition will be horizontally fixed, representing the stable wall. Hence it will allow movements vertically but constrain horizontal displacements as well. Y-min will be totally fixed, meaning no movement from the ground surface (bedrock level). Y-max will be set free for proper displacement after applying the normal load at the footing.
6. At the stage of construction, an individual phase is created for every layer that will cover the spacing. The block and the respective interface are activated for the soil placement phase. After placing the first layer, the following phase should include the compaction load and continue with the next layer.

Figure 3.33 shows the construction phase of the first layer.

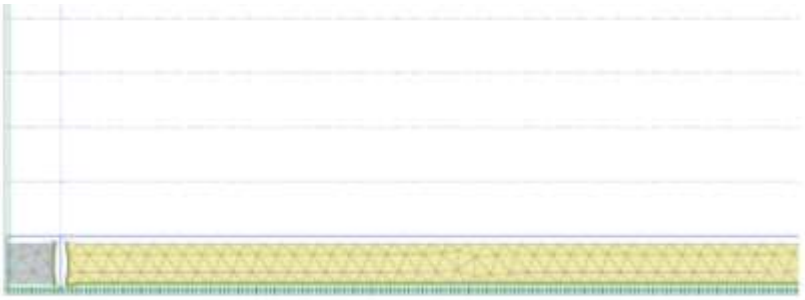

Figure 3.3: Construction phase of the first layer.

7. Additionally, the geogrid feature must be activated once the construction phase reaches a geosynthetic layer.
8. Once all the layers are activated, the x-min boundary condition is changed to totally free, allowing free movement in front of the wall.
9. Activate the normal load at the desired level. The lowest value used for the study is 12 kPa for traffic load representation until reaching 3000kPa. On the other hand, the wall example following Huang et al. (2009) will follow increments of 10 kPa.
10. Inspect the results and interpretation for horizontal and vertical lateral deformation, failure plastic points, and vertical and horizontal stress generation. Furthermore, the hardening of the soil can be visualized throughout the construction phases.

Figure 3.4 shows the primary results window showing the mesh deformation.

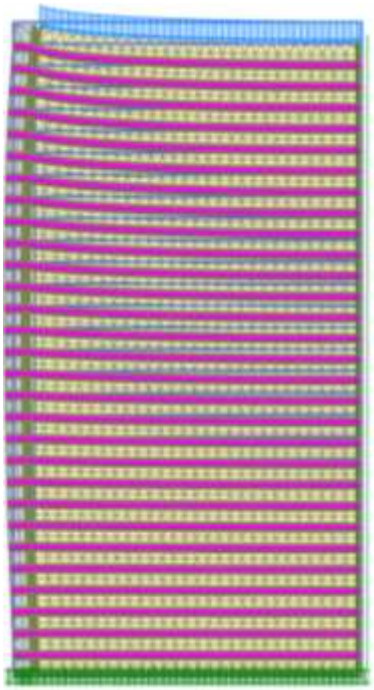

Figure 3.4: Deformed mesh of 0.5 L/H Wall with a spacing of 0.2m at 200kPa Normal Test

CHAPTER IV

RESULTS AND DISCUSSION

Chapter IV covers the parametric study of 0.5 L/H narrow MSE walls and 0.3 L/H NMSE wall models under several reinforcement configurations with the assistance of the program PLAXIS 2D. Other factors considered in the study are increased tensile reinforcement strength and different narrow MSE wall ratios. The models' primary focus will be identifying the effect of secondary reinforcements in narrow MSE walls, analyzing the ideal case for using secondary reinforcement, and what ratio will be more beneficial for narrow MSE walls. Before proceeding with the parametric study, a numerical model of Huang et al. (2009) wall 1 is simulated using the Hardening soil model to calibrate the program with laboratory testing. The comparison between both tests confirms the ability of PLAXIS 2D to replicate reinforcing soil technology cases. Furthermore, 14 main models were generated with the assistance of PLAXIS 2D as part of the parametric study, where their description is illustrated in tables 4.1 and 4.2. Analysis of the test results will be complemented under the discussion of the model, and graphs will assist in visualizing the improvement of reinforcement configuration under identical load conditions.

4.1 MSE and NMSE Modeling

Huang et al.'s (2009) MSE wall is selected to use as an example of numerical modeling capabilities, where surcharge loads were applied in a 10 kPa sequence. The test wall from the article chosen was constructed and monitored with the assistance of more than 300 instruments located at strategic points of the MSE wall configuration. Moreover, the wall selected was built on a rigid foundation of 3.6 meters in height and 6 meters wide from the fall facing and named wall 1. Concrete blocks were used for the MSE wall facing, and the respective properties were also used in the model. Moreover, the wall has a target batter of 8 degrees, challenging the interaction between the blocks and the soil material for the model interface. For the geosynthetic material used, weak biaxial punched and drawn polypropylene (PP) geogrid is applied.

Regarding the mechanical behavior of the soil, Hardening Soil Model was used, while Mohr-Coulomb Model was applied for the interface materials. In addition, a linear elastic model was implemented for the geogrid modeling. Once all the properties were involved in the numerical model, surcharge loads of 8 kPa were applied during the construction phases of the layers, replicating the compaction loads applied in every wall layer. Once the wall was constructed, loads of 10 kPa increments were applied on top for further study. Figure 4.1 shows the PLAXIS model meshing of Huang et al.'s (2009) wall.

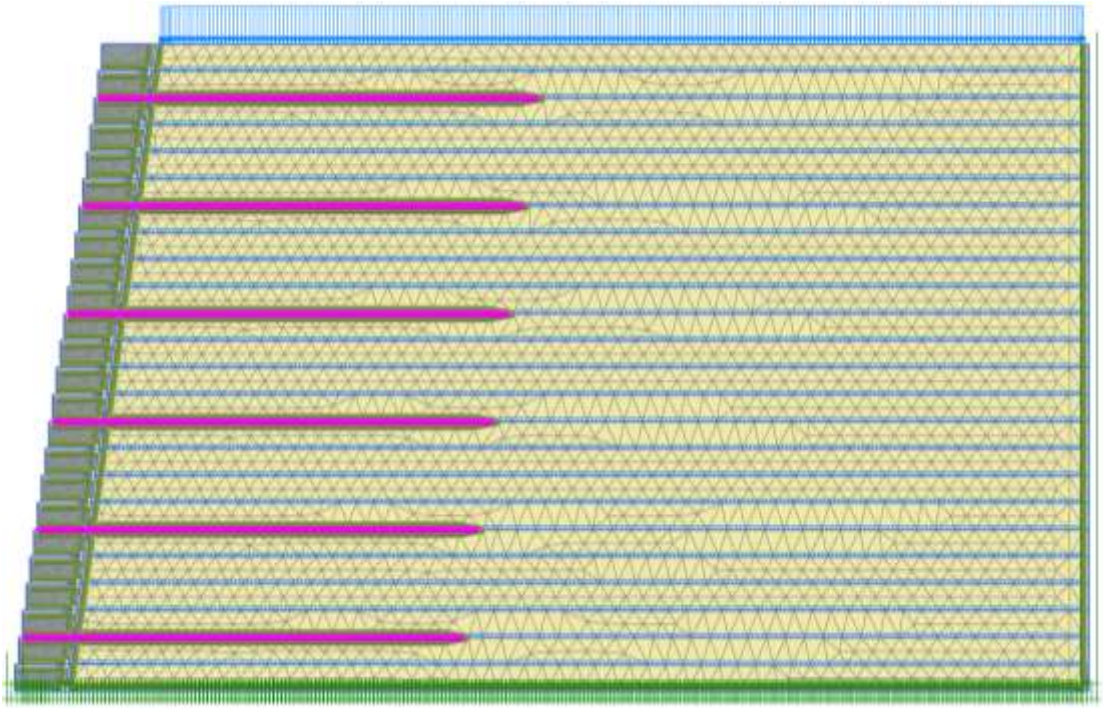

Figure 4.1: PLAXIS model of Huang et al. (2009) full-scale wall

Loads increments continued until the calculation process ended. From the calculation feature, several tools are available to visualize the results. Figure 4.2 shows the lateral displacement of the Huang's wall and the PLAXIS model. Good agreement between the numerical model and the Full-scale model is show in the figure confirming the use of PLAXIS for modeling the NMSE walls for this study.

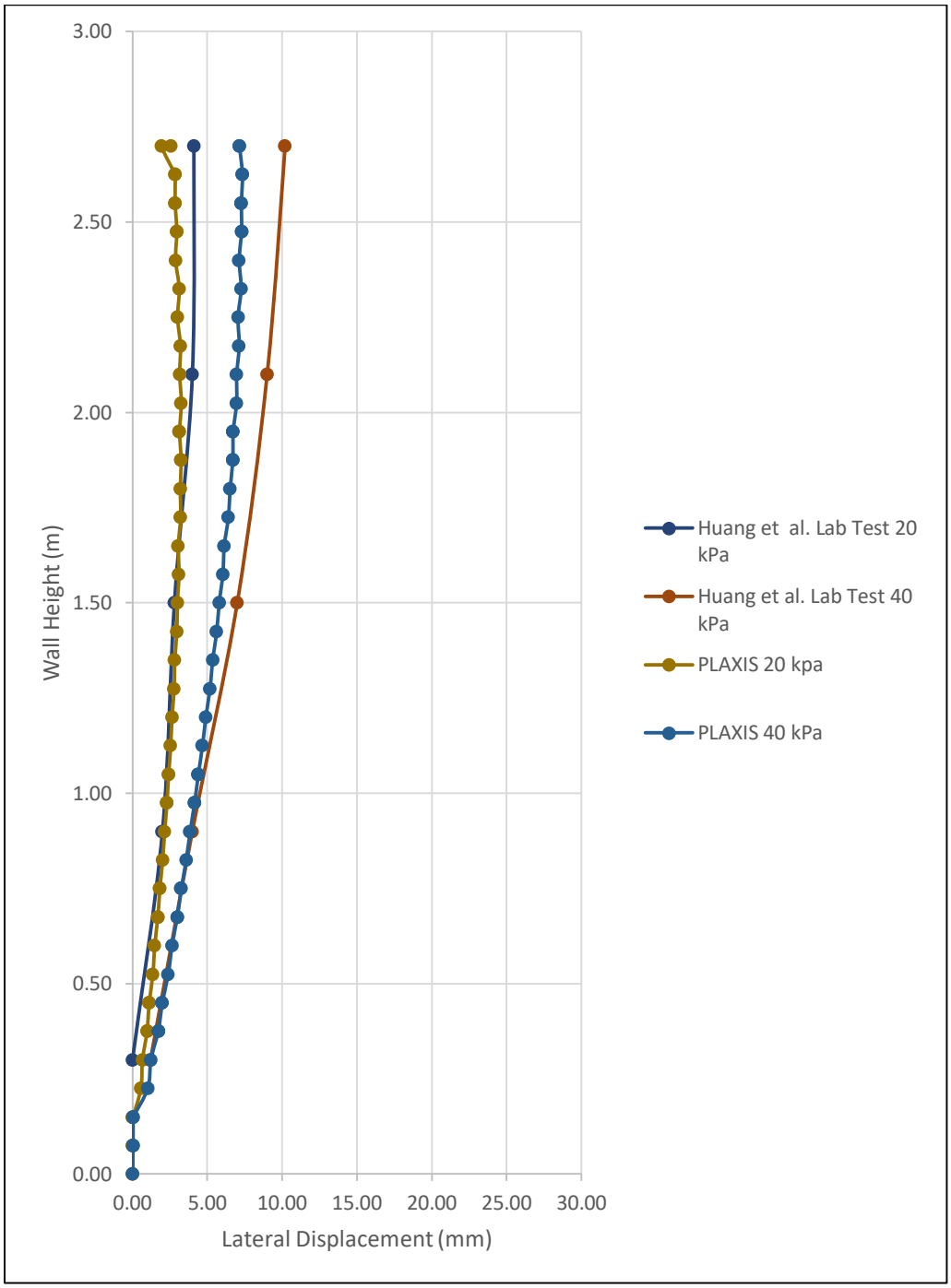

Figure 4.2: Lateral displacement comparison of Huang's Wall and PLAXIS model

4.2 Secondary Reinforcement Configuration

For this study, adequate conditions to add secondary reinforcement layers were proposed to reduce the amount of reinforcement and increase the performance of the NMSE walls. Narrow walls of 6 meters in height by 3 meters wide are modeled with several reinforcement configurations. Moreover, an additional narrow wall of 0.3 L/H ratios is used for soil behavior comparison. Models 1 through 7 follow a length-to-height ratio of 0.5, which is considered in the range of narrow MSE walls. Models 1 through 4 will have primary reinforcement configurations at different spacing (figure 4.3), while models 5 through 7 will include secondary reinforcement addition at different spacing, as shown in figure 4.4. Model 8 will have a 0.3 L/H ratio, the smallest ratio used for this analysis. See figure 4.5 for reference. Table 4.1 shows the reinforcement configuration for the first eight models. Moreover, an additional model will be included for the effect of reinforcement with a double increase in strength, and models with a reduction in reinforcement length are also used as part of the study. Table 4.2 shows the model configuration for different reinforcement lengths used for a 0.5 L/H Wall with primary reinforcement of 0.4m, and figure 4.6 illustrates this model. Moreover, table 4.3 shows the number of tests required to be made depending on the model used. Lastly, Table 4.4 displays the number of geosynthetics used per model in the meter's unit. For example, model 1 required 29 geosynthetic layers of 3 meters long since it only uses primary reinforcement with spacing for every block increment. Hence, requiring a total of 87 meters of reinforcement material.

A total of 6 tests were conducted to analyze NMSE behavior with the addition of secondary reinforcement. Test 1 focuses on traffic loads application on the retained backfill soil. Models 1 through 8 will serve for these tests. Test 2 will analyze the large primary reinforcement spacing effect with the addition of secondary reinforcement configuration. For this test, models 6 and 7 are used.

Moreover, test 3 focuses on the L/H ratio wall comparison between 0.5 and 0.3 using models 7 and 8. The 0.3 L/H wall will only have primary reinforcement, while the 0.5 L/H wall counts with secondary reinforcement. Test 4 includes models 9 through 14 for analyzing the reinforcement length effect with high surcharge loads applied. Also, model 5 is used again in this model with a reinforcement length of 1.5 m. Hence, the proper reinforcement length for narrow walls can be observed. Test 5 focuses on the reinforcement quantity used per mode. Lastly, test 6 compares the efficiency of using stronger reinforcement against weaker reinforcement with secondary layers

Table 4.1 Numerical Model Configuration

Model	Primary Reinforcement Spacing	Secondary Reinforcement Spacing	L/H Ratio
1	0.2	-	0.5
2	0.4	-	0.5
3	0.3	-	0.5
4	0.6	-	0.5
5	0.4	0.2	0.5
6	0.6	0.2	0.5
7	0.6	0.3	0.5
8	0.2	-	0.3

Table 4.2 Test 4 Reinforcement Length Configuration

Model	Secondary Reinforcement (m)
9	0.40
10	0.60
11	0.80
12	1.00
13	1.20
14	1.80

Table 4.3 Total Number of Tests

Model	Number of Tests
1	9
2	5
3	4
4	11
5	5
6	5
7	5
8	5
9	9
10	4
11	4
12	4
13	4
14	1
Total	75

Table 4.4 Reinforcement Material Comparison

Material Required	
Model	Geosynthetics(m)
1	87
2	42
3	27
4	27
5	64.5
6	57
7	42
8	52.2
9	48
10	51
11	54
12	57
13	60
14	69

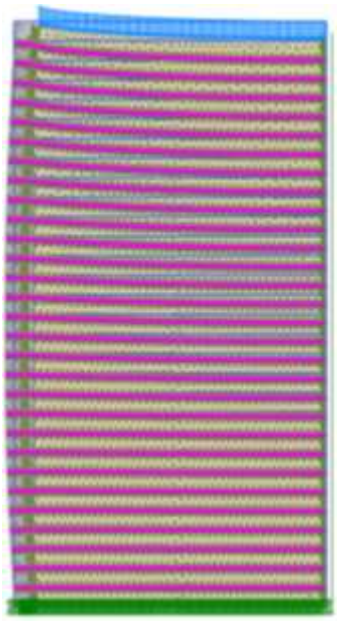

Model 1

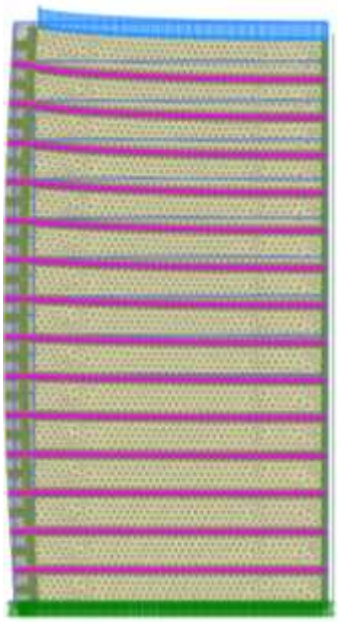

Model 2

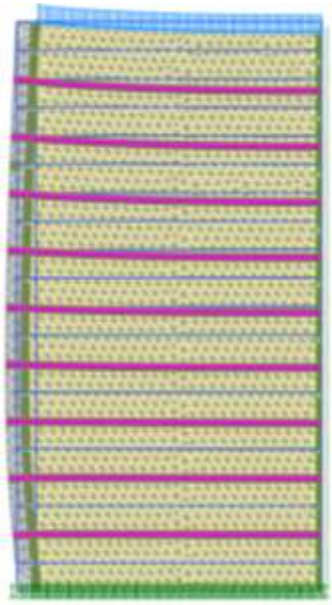

Model 3

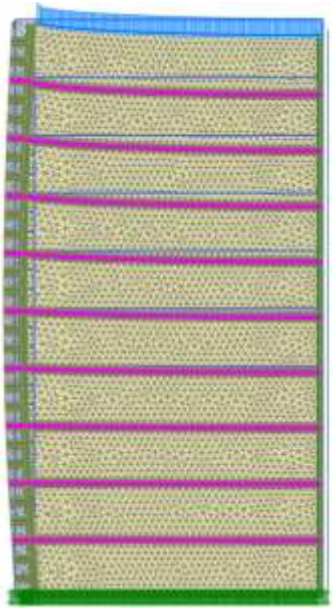

Model 4

Figure 4.3: Models with primary reinforcement only

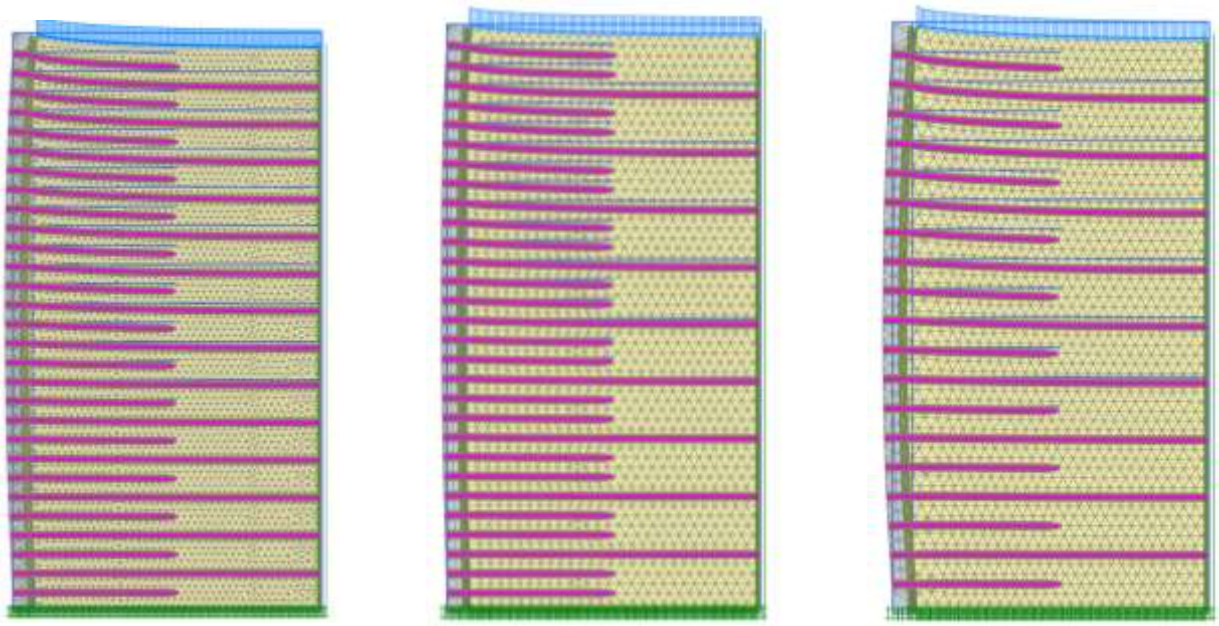

Model 5 Model 6 Model 7

Figure 4.4: Models with the addition of secondary reinforcement

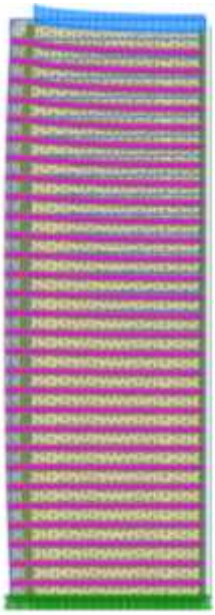

Model 8

Figure 4.5: Model with an L/H ratio of 0.3

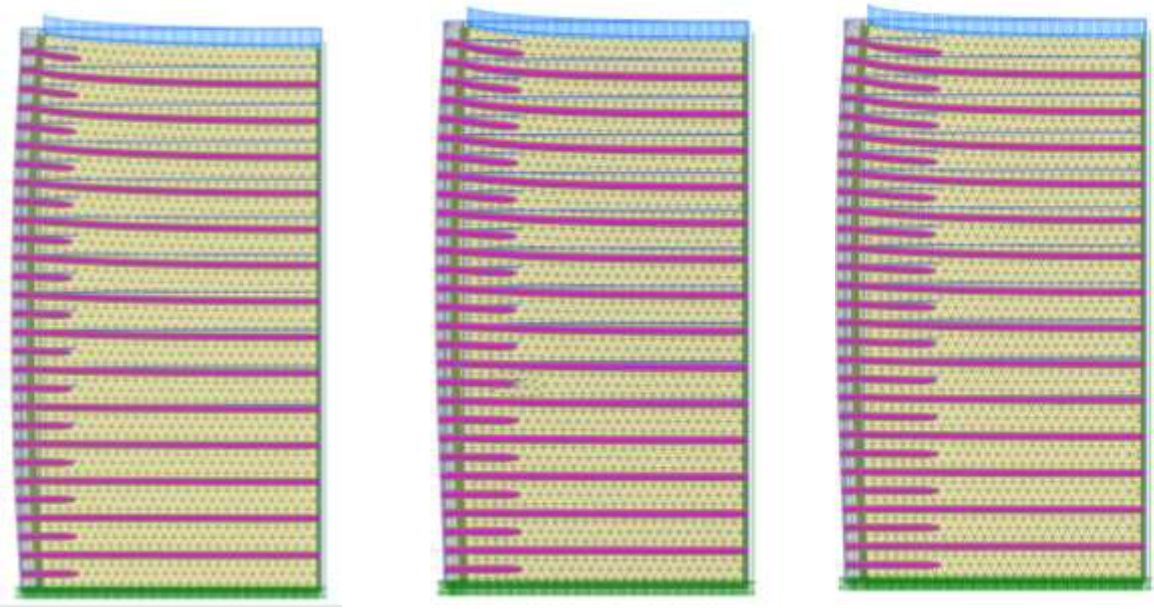

Model 9 Model 10 Model 11

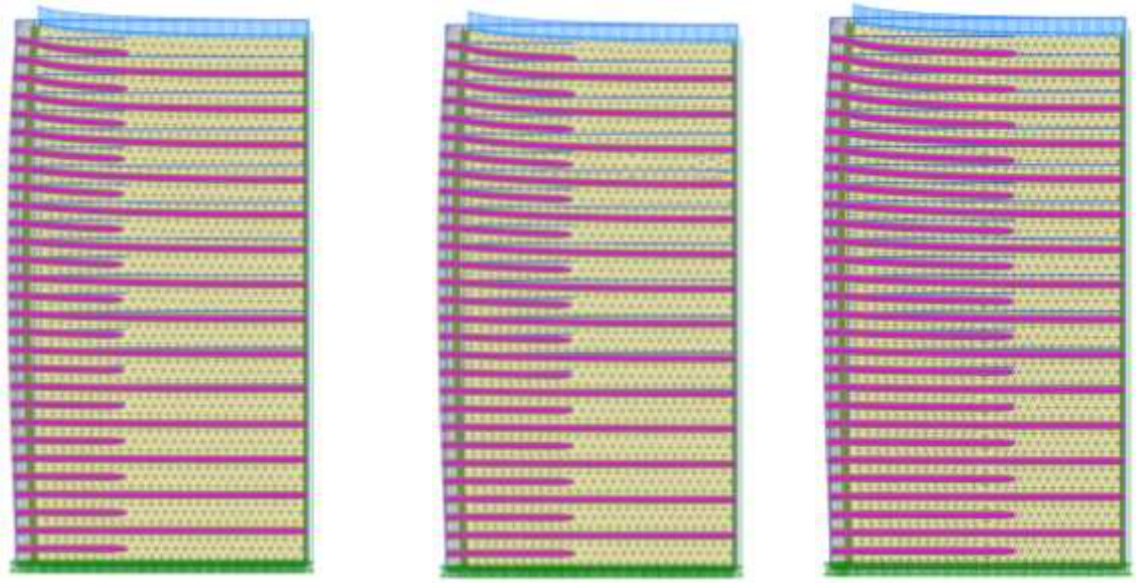

Model 12 Model 13 Model 14

Figure 4.6: Models with different reinforcement lengths with an L/H ratio of 0.5

4.3 Test 1: Traffic Load Analysis

NMSE walls retain soil or support pavement/roadway in narrow areas. Demand for NMSE walls increases in areas where narrow natural conditions are common. Therefore, the recommended reinforcement length-to-height ratio of 0.7 is impossible in this narrow area. Besides preliminary reinforcement layers, secondary reinforcement layers are added to increase the wall's local and overall stability and performance. Moreover, the reinforced backfill soil must withstand the recommended design load of 250 psf as given by ASHTO guidelines. In this study, a comparison of several wall configurations is used to see the behavior of wall displacement concerning traffic load. This model will contribute to observing the performance of geosynthetic material used depending on the model's configuration.

Figure 4.7 shows the comparison of models 1 and 8 for applying traffic loads on top of the wall, and figure 4.8 shows the comparison of the first 8 models. A surcharge load of 12 kPa is applied following the AASHTO guidelines. Both figures show how model 8 obtained a less lateral displacement of 0.7mm with primary reinforcement at every block layer of the 0.3 L/H walls compared to model 1. Models 1,2,3,4,5 and 7 almost acquire the same displacement pattern, while model 6 resulted in the more significant displacement from all the models. A comparison of models 1 and 8 gives a 31.36% less maximum lateral displacement and 44.52% less maximum displacement comparing model 8 with model 6. This test clearly shows how all the models can withstand traffic loads with minimal lateral displacement. Furthermore, local stability can be observed as the models with secondary reinforcement also obtained equal displacement without failure.

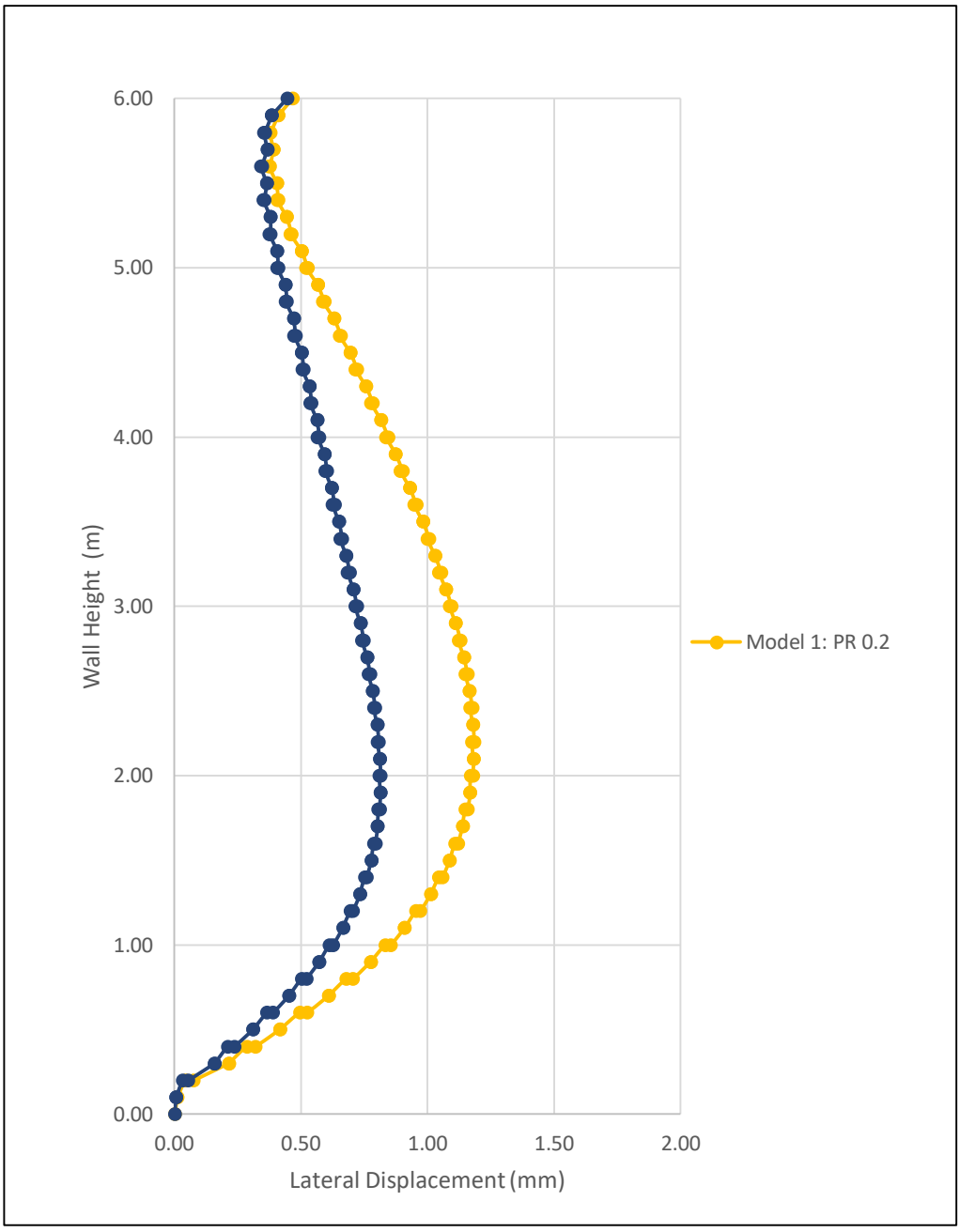

Figure 4.7: Traffic load analysis of models 1 and 8. (PR): Primary Reinforcement / (SR): Secondary Reinforcement / (L/H): Length to Height Ratio.

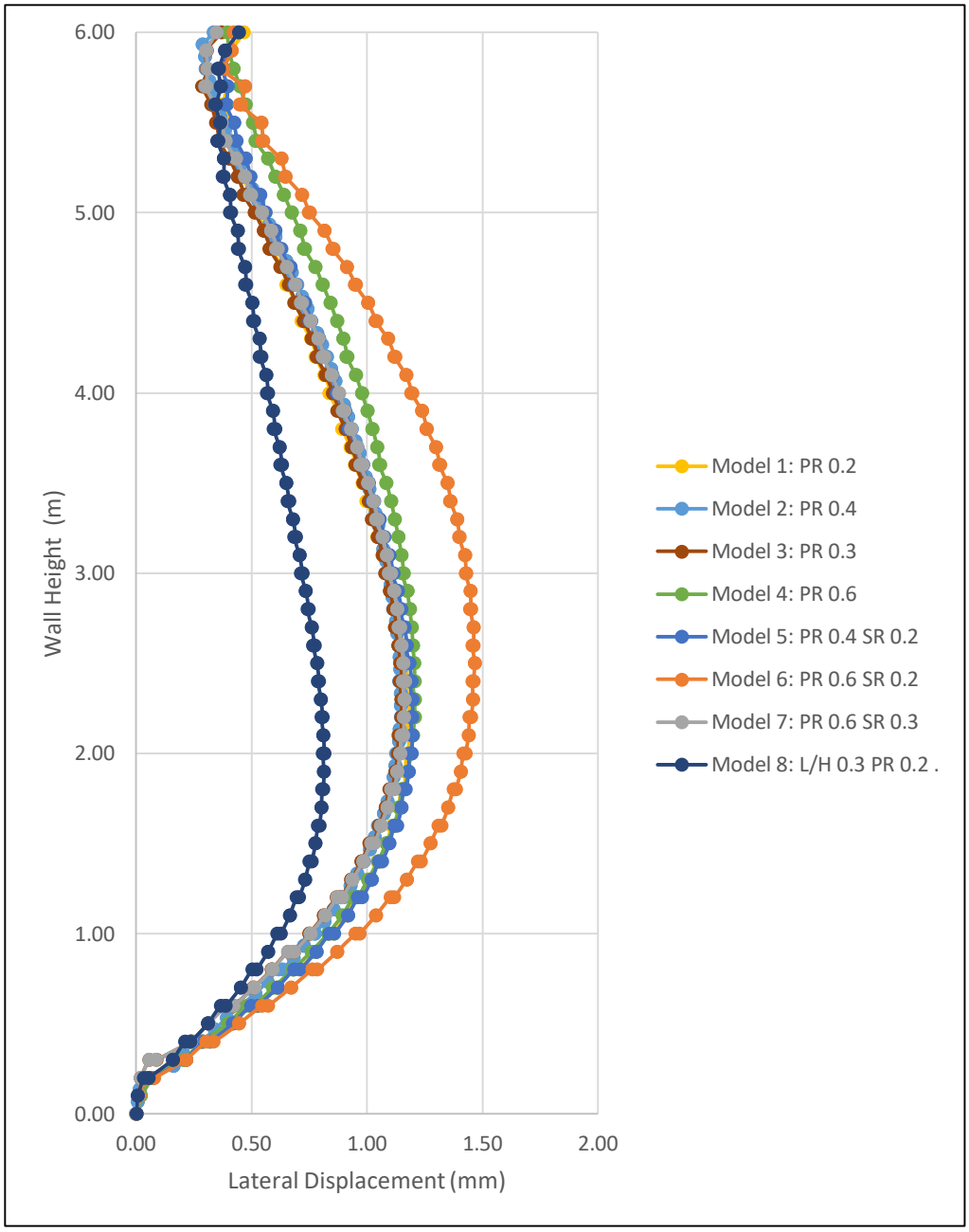

Figure 4.8: Traffic load analysis test for models 1 through 8.

Moreover, the less lateral displacement from model 8 can be attributed to the smaller spacing used than in the other models. This confirms previous studies such as Broms (1977), Woodruff (2003), Vulova and Leshcinsky's (2003), Elton and Patawanran (2005), Pham (2009), Karakasul (2018) made on MSE walls under normal conditions and contributes to confirming the NMSE wall performance under traffic loads. It must be mentioned that this model applies to modular block facing, and unequal wall configuration may not be applicable, such as using wrapped around facing wall. Moreover, the fact that all models fall into the same displacement range means that an increase in surcharge load can continue until maximum load capacity per model is obtained.

4.4 Test 2 Secondary Reinforcement Comparison Test

The following test compares the use of 2 or 1 secondary reinforcement layer between the primary reinforcements. For this reason, models 6 and 7 are suitable for application in this test since both have the same primary reinforcement with sufficient space to add either 1 or 2 secondary reinforcement layers. Figure 4.9 shows the comparison of models 6 and 7 in the 0.5 L/H walls category. From the figure, both walls obtained similar displacement at the 44kPa and 100kPa tests. However, the model with 1 secondary reinforcement begins to displace at a greater scale after a significant surcharge load is applied. This is the case for the 200 and 300 kPa tests. In terms of geosynthetic material use, model 6 uses 19 reinforcement layers equivalent to 57 meters of material, while model 7 only uses 42 meters. Even though model 7 acquired a larger displacement, the maximum difference in the 300 kPa test is 5 mm. Reducing to 1 secondary reinforcement instead of 2 can still be eligible to perform safely with a material reduction since both models did not reach failure.

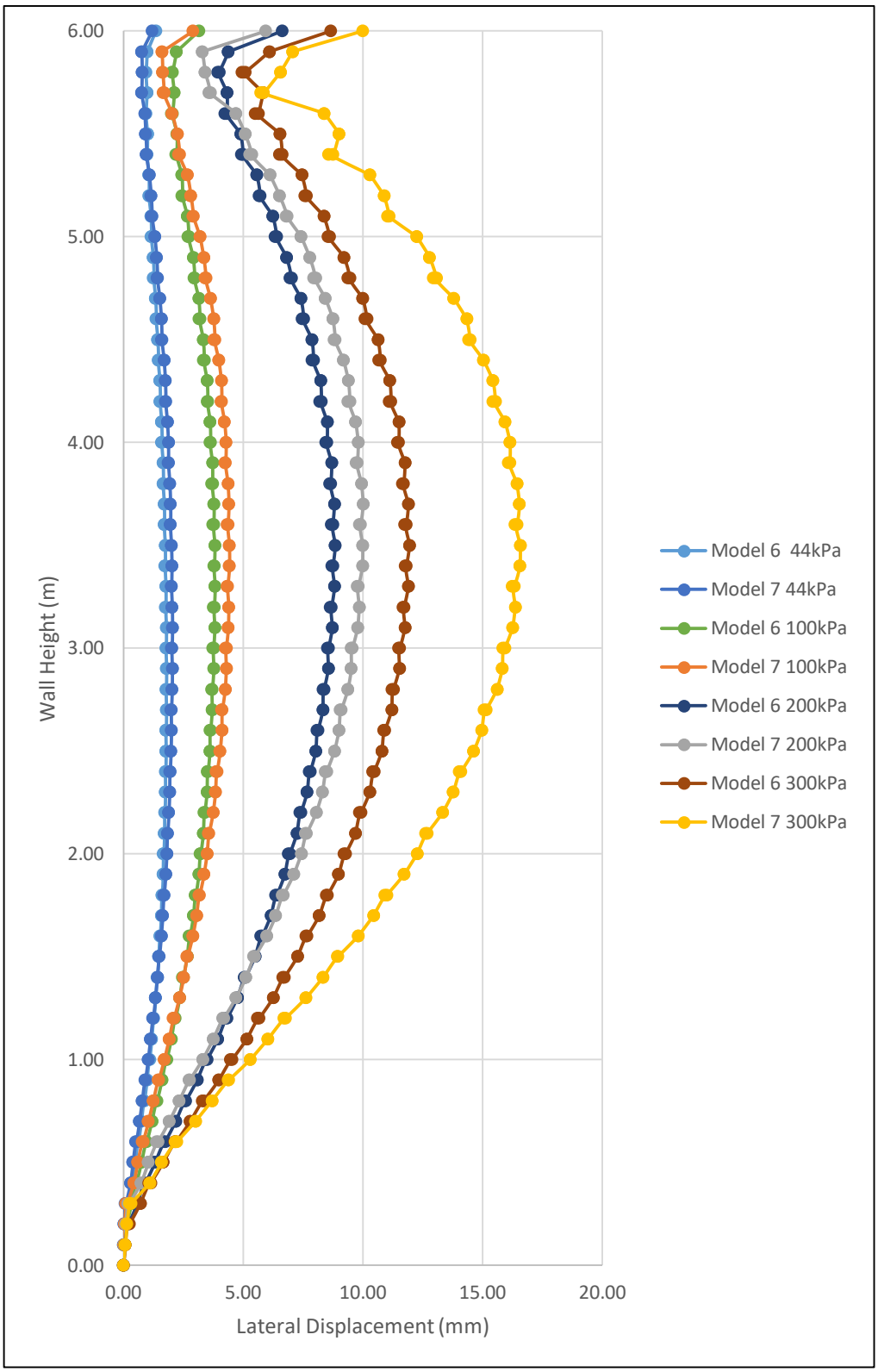

Figure 4.9: Secondary reinforcing spacing test results.

4.5 Test 3: Length to Height Ratio Test

Test 3 focuses on the performance of walls with 0.5 and 0.3 L/H ratios. Models 7 and 8 are chosen for this test since model 8 represents the narrowest model with close spacing. Model 7 was selected since it represents a 0.5 L/H wall with greater primary spacing and enough space to include secondary reinforcement. Therefore, it will assist in comparing which wall has greater efficiency in either using secondary reinforcements or closer primary spacing. Figure 4.10 shows the results from applying surcharge loads up to 300 kPa. The calculation results in figure 4.10 clearly show model 8 acquiring less displacement than expected due to the close spacing of the reinforcement regardless of the dimensions. Test at 300 kPa presents a noticeable change in behavior from model 7 to 8. Furthermore, it resembles the behavior seen in test number 1. Again, spacing is still playing a significant factor in the internal stability of the wall.

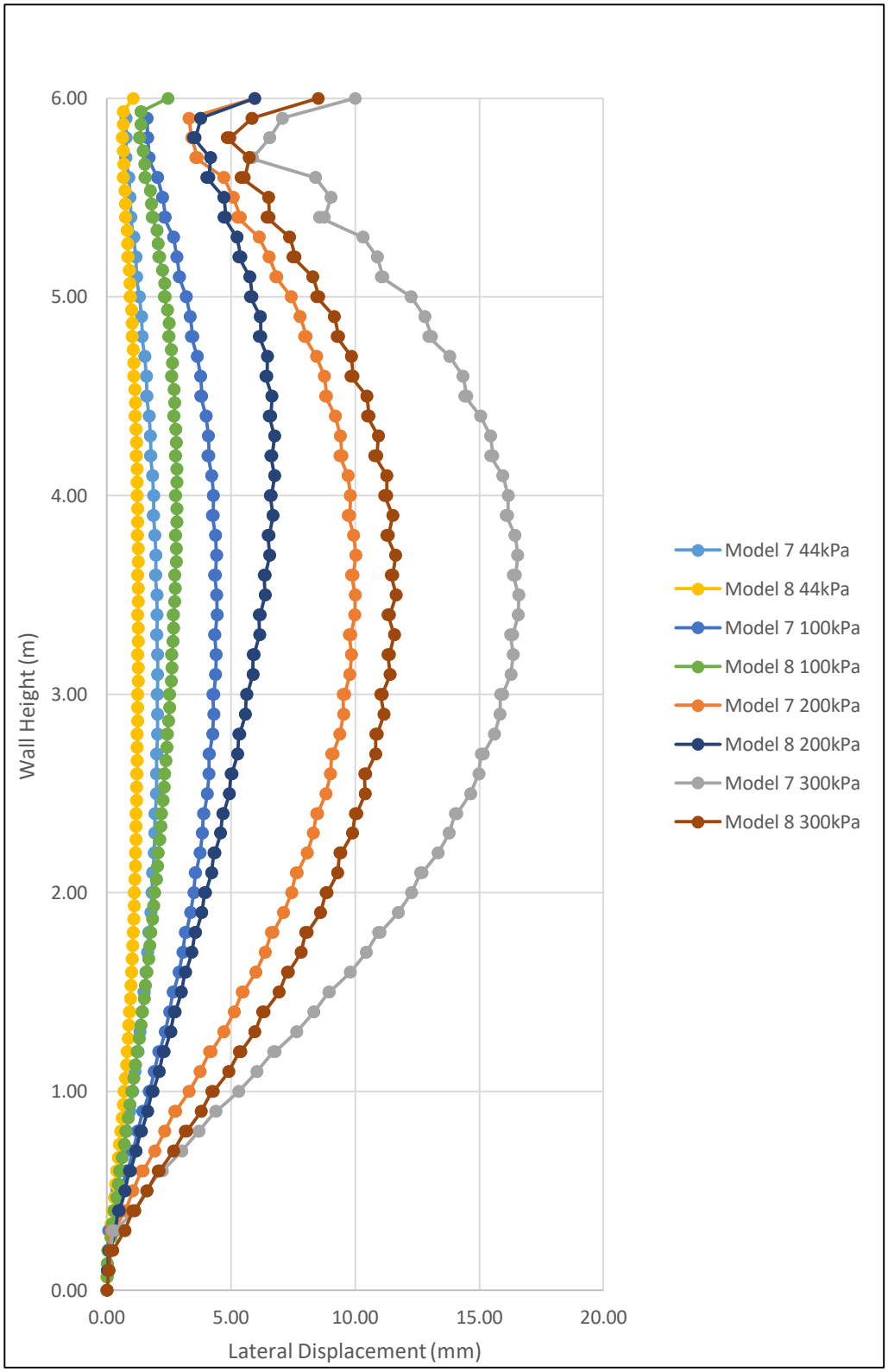

Figure 4.10: Length to height ratio test results

4.6 Test 4: Reinforcement Length Comparison

Test 4 focuses on applying different reinforcement lengths to observe the performance of the wall while reducing the material used. The reinforcement length used for this test is given in table 4.2, and model 5 was used again for the maximum secondary reinforcement length. Figure 4.11 shows the results after a surcharge load of 200 kPa was applied to models 9 through 14 and 5. Figure 4.12 shows the maximum lateral displacement achieved in every model according to the reinforcement length. Figure 4.11 shows a slight difference in lateral displacement in all models. This difference is virtually 0 since it does not pass to the units of millimeters. Hence the model with less reinforcement length can perform under similar conditions to the model with greater length. In terms of material use, there is a reduction of 30.43% of reinforcement use compared to model 9 with model 14.

On the other hand, figure 4.12 shows a tendency to achieve a static value for maximum lateral deformation when reinforcement length reaches 1.2m. Therefore, this point may be defined as the secondary reinforcement length limit to achieve equal deformation. For future studies, an equation that could predict this behavior will contribute to refining this study.

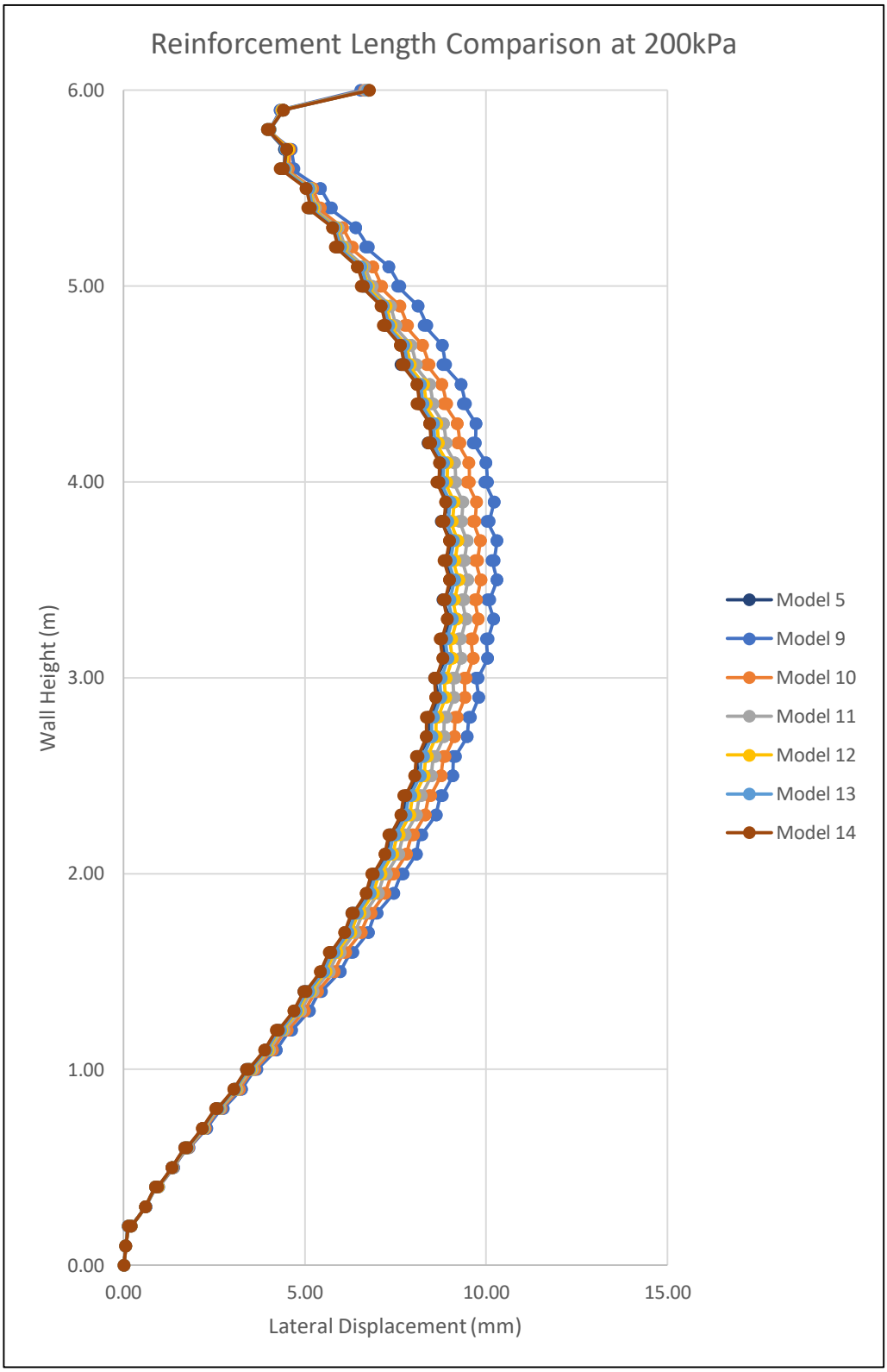

Figure 4.11: Reinforcement length test results

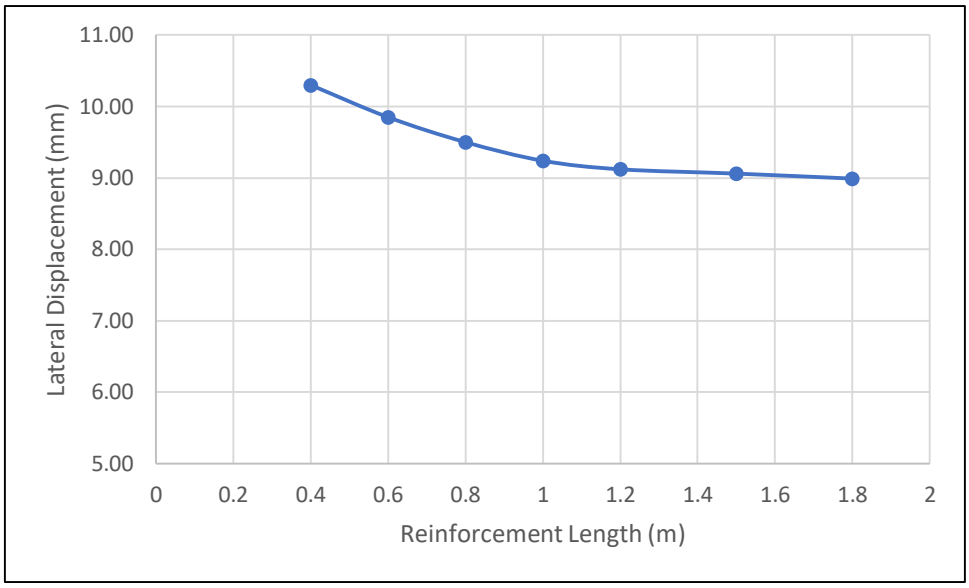

Figure 4.12: Maximum lateral displacement test results at 200kPa.

4.7 Test 5: Geosynthetic Material Use Test

Test number 5 focuses on the number of geosynthetic materials used depending on the wall's reinforcement configuration. Therefore, this test requires the same L/H ratio for the models to account for the comparison. Models 1, 5, and 6 are selected for the evaluation due to the similarity in dimensions with unequal distribution of reinforcement material. Model 1 uses 87m of material, while model 5 uses 64.5m, and model 6 uses 57m. Figure 4.13 shows the results of these tests at several surcharge loads applied. From the results, the model with just one secondary reinforcement layer between primary reinforcement (model 5) acquired less displacement than models 1 and 6. Even though model 5 uses a mayor number of geosynthetic materials in comparison with model 6, the difference is minimal. Hence, the configuration of model 5 can be used instead of model 6 for secondary reinforcement addition.

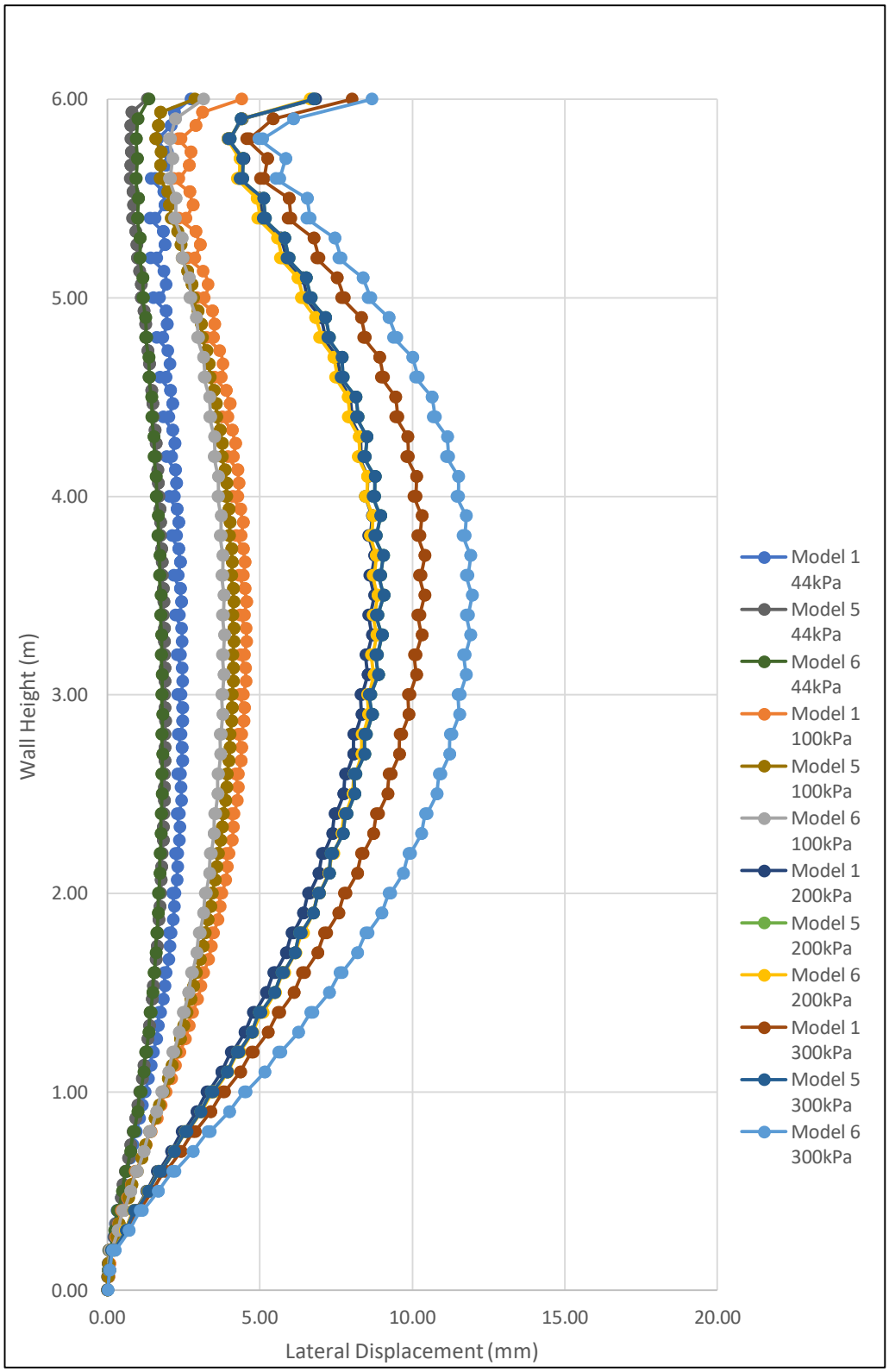

Figure 4.13: Geosynthetic usage comparison

This study concludes with a decrease in material use of 34.48% in the case of performing under similar conditions and 25.86% in greater conditions.

4.8 Test 6: Reinforcement Tensile Strength Test

Lastly, a test focusing on the performance of NMSE walls with stronger reinforcement is compared with a regular secondary reinforcement model. Both models must have the same wall dimensions and equal primary reinforcement spacing, giving the parameter of adding secondary reinforcement for one model and the other increasing the strength value of the reinforcement. Hence, models 6 and 4 are selected for this test, where reinforcement in model 4 is increased to a factor of 2 using only primary reinforcement. Model 6 is characterized by secondary reinforcement at 0.2m and primary spacing at 0.6m. Figure 4.14 shows the results of different surcharge loads applied to both models. The figure shows that regardless of increasing the tensile strength of the primary reinforcement of model 4, model 6 achieves less lateral displacement. Hence, it proves the importance of spacing rather than strength in reinforcement for narrow MSE walls.

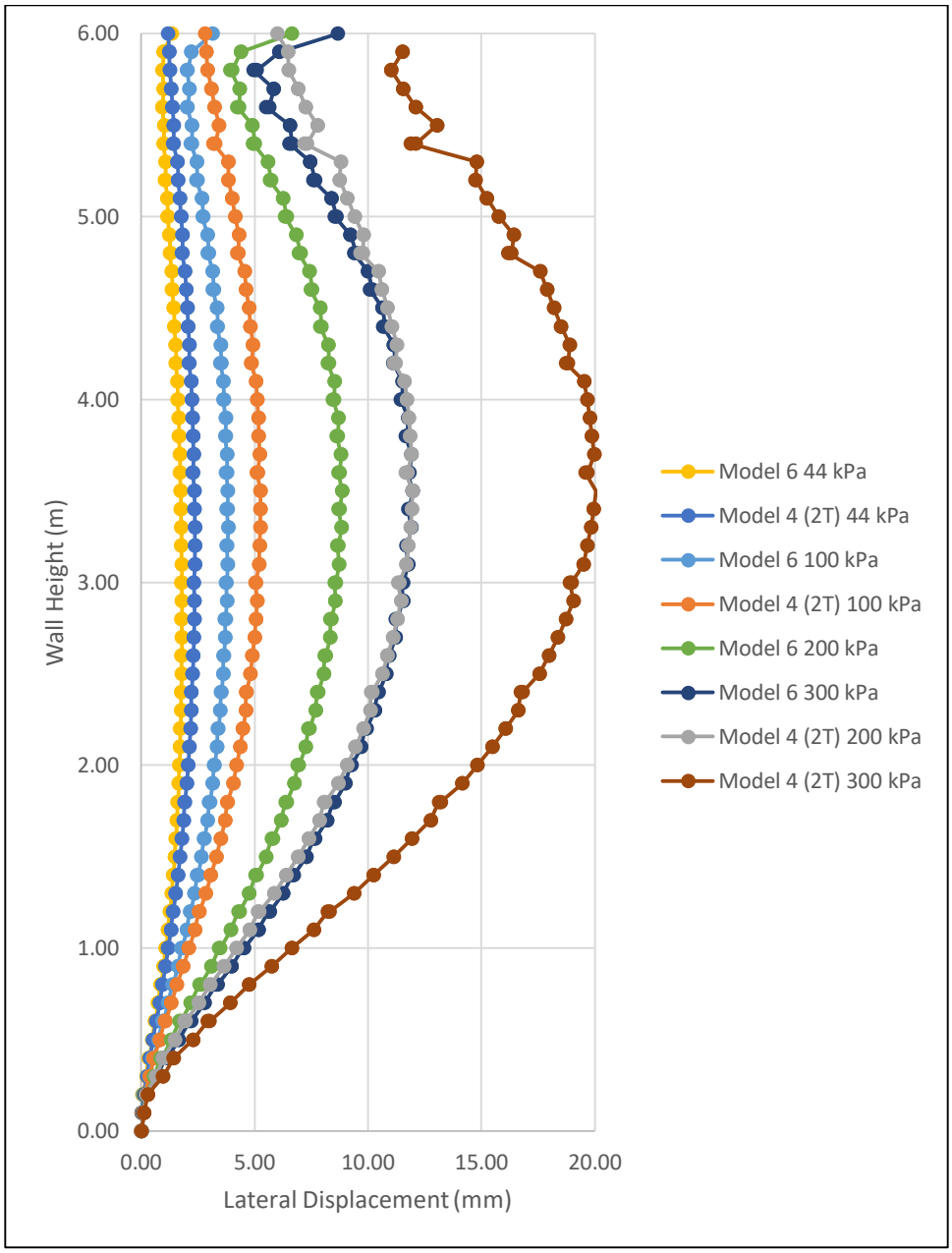

Figure 4.14: Reinforcement tensile strength test results

CHAPTER V

CONCLUSIONS

Several FEM models were developed using PLAXIS2D to study the relationship between secondary reinforcements and Length to Height Ratio of NMSE walls. The Hardening soil model was utilized to simulate the soil behavior, and interfaces between the materials were included for refining the models. The conclusions of this study are summarized as follows

1. Smaller spacing on a 0.3L/H wall contributed to more excellent wall stability, up to 31.36% more benefit than the 0.5 L/H model under traffic load conditions.
2. 0.5 L/H NMSE walls with secondary reinforcement and 0.3 L/H NMSE walls without secondary reinforcement can withstand traffic loads. This case applies to modular block-facing walls and may not apply to other designs.
3. Smaller spacing at secondary reinforcement layers contributes to a decrease in lateral displacement. However, using 1 secondary reinforcement layer can also perform in good conditions at high surcharge loads regardless of the material use difference.
4. Reinforcement spacing plays a more significant role in local stability than secondary reinforcement for NMSE walls under high surcharge load conditions.
5. Reinforcement length performs in similar conditions under high surcharge loads regardless of how much material is intended to use. 30.43% of material reduction is obtained while achieving equal maximum lateral displacement. Moreover, a tendency to

6. attain the same maximum lateral displacement can be found at a certain length. Thus, creating a secondary reinforcement length limit.
7. The use of secondary reinforcement reduces the amount of geosynthetic material required to perform in similar or better conditions than using primary reinforcement. A 34.48% reduction can be achieved for similar results and 25.86% for better results.
8. Spacing in NMSE walls has greater performance than reinforcement strength.

REFERENCES

Adams, Michael T., and James G. Collin. "Large model spread footing load tests on geosynthetic reinforced soil foundations." *Journal of geotechnical and geoenvironmental engineering* 123.1 (1997): 66-72.

Broms, Bengt B. "Triaxial tests with fabric-reinforced soil." *CR Coll. Int. Soils Textiles* (1977): 129-133.

Budge, Aaron S., James A. Bay, and Loren R. Anderson. "Calibrating vertical deformations in a finite element model of an MSE wall." *GeoCongress 2006: Geotechnical Engineering in the Information Technology Age*. 2006. 1-5.

Chen, Qiming, Murad Abu-Farsakh, and Radhey Sharma. "Experimental and analytical studies of reinforced crushed limestone." *Geotextiles and Geomembranes* 27.5 (2009): 357-367.

Christopher, Barry R., and Victor Elias. *Mechanically Stabilized Earth Walls and Reinforced Soil Slopes Design and Construction Guidelines*. No. FHWA-SA-96-071. United States. Federal Highway Administration, 1997.

Duncan, James M., and Chin-Yung Chang. "Nonlinear Analysis of Stress and Strain in Soils." *Journal of the Soil Mechanics and Foundations Division*, vol. 96, no. 5, 1970, pp. 1629–1653., https://doi.org/10.1061/jsfeaq.0001458

Elton, David J., and Maria Aries Barrato Patawaran. "Mechanically stabilized earth (MSE) reinforcement tensile strength from tests of geotextile reinforced soil." *Alabama Highway Research Center, Auburn University* (2005).

Frydman, Sam, and Israel Keissar. "Earth pressure on retaining walls near rock faces." *Journal of Geotechnical Engineering* 113.6 (1987): 586-599.

Han, Jie, et al. "Fully-mobilized soil arching versus partially-mobilized soil arching." *Proc., 2016 Int. Conf. on Transportation Infrastructure and Materials*. 2016.

Han, Jie, et al. "Progressive development of two-dimensional soil arching with displacement." *International Journal of Geomechanics* 17.12 (2017): 04017112.

Hegde, A., Roy, R. A Comparative Numerical Study on Soil–Geosynthetic Interactions Using Large Scale Direct Shear Test and Pullout Test. *Int. J. of Geosynth. and Ground Eng.* **4,** 2 (2018). https://doi.org/10.1007/s40891-017-0119-1

Hossain, M. S., et al. “Effects of Backfill Soil on Excessive Movement of MSE Wall.” *Journal of Performance of Constructed Facilities*, American Society of Civil Engineers, 18 Aug. 2011, ascelibrary.org/doi/abs/10.1061/%28ASCE%29CF.1943-5509.0000281

Huang, Bingquan, Richard J. Bathurst, and Kianoosh Hatami. "Numerical study of reinforced soil segmental walls using three different constitutive soil models." *Journal of Geotechnical and Geoenvironmental engineering* 135.10 (2009): 1486-1498.

Jarrett, N. D., C. J. Brown, and D. B. Moore. "Pressure measurements in a rectangular silo." *Geotechnique* 45.1 (1995): 95-104.

Jiang, Yan, et al. “Field Monitoring of Mechanically Stabilized Earth Walls to Investigate Secondary Reinforcement Effects.” *Welcome to ROSA P*, Kansas. Dept. of Transportation. Bureau of Research, 1 Dec. 2015, https://rosap.ntl.bts.gov/view/dot/29651

Kniss, Ken T., et al. "Earth pressures and design considerations of narrow MSE walls." *Proceedings of the Texas Section ASCE Spring Meeting*. 2007.

Koerner, R. M. (1997). Designing with Geosynthetics/ 4th ed., Pearson, 1997.

Kakrasul, Jamal Ismael. “Geosynthetic Reinforced Retaining Walls with Limited Fill Space under Static Footing Loading.” *KU ScholarWorks*, University of Kansas, 31 May 2018, kuscholarworks.ku.edu/handle/1808/27592.

Koerner. R. M. (1997). Designing with Geosynthetcics/ 4th ed., Pearson, 1997.

Lawson, C. R., and T. W. Yee. "Reinforced soil retaining walls with constrained reinforced fill zones." *Slopes and Retaining Structures Under Seismic and Static Conditions*. 2005. 1-14.

Leshchinsky, D. (2000). Alleviating connection load. Geotechnical Fabrics Report, 18(8), 34-39.

Leshchinsky, D., and C. Vulova. “Numerical Investigation of the Effects of Geosynthetic Spacing on Failure Mechanisms in MSE Block Walls.” *Geosynthetics International*, vol. 8, no. 4, 2001, pp. 343–365., https://doi.org/10.1680/gein.8.0199

Leshchinsky, Dov, et al. “Framework for Limit State Design of Geosynthetic-Reinforced Walls and Slopes.” *Transportation Infrastructure Geotechnology*, vol. 1, no. 2, 2014, pp. 129–164., https://doi.org/10.1007/s40515-014-0006-3

Ling, H. I., et al. "Finite element study of a geosynthetic-reinforced soil retaining wall with concrete-block facing." *Geosynthetics International* 7.3 (2000): 163-188.

LUO, Yu-Shan, XU Chao, Bin JIA, Hong-shuai CHEN, Centrifuge modeling of shored MSE walls with different interface connections, Laboratory of Geotechnical and Underground Engineering of Ministry of Education. September 2014.

Mahmood, Tahsina. *Failure analysis of a mechanically stabilized earth (MSE) wall using finite element program Plaxis*. Diss. The University of Texas at Arlington, 2009.

Michalowski, Radoslaw L. "Secondary Reinforcement for Slopes." *Journal of Geotechnical and Geoenvironmental Engineering*, vol. 126, no. 12, 2000, pp. 1166–1173., https://doi.org/10.1061/(asce)1090-0241(2000)126:12(1166).

Morrison, Kimberly Finke, et al. *Shored mechanically stabilized earth (SMSE) wall systems design guidelines*. No. FHWA-CFL/TD-06-001. United States. Federal Highway Administration. Central Federal Lands Highway Division, 2006.

Derrick, Nasasira, and Amit Kumar Srivastava. "Effect of mesh size on soil-structure interaction in finite element analysis." *Int J Eng Res Technol* 9.06 (2020).

Pham, Thang. (2009). Investigating Composite Behavior of Geosynthetic-Reinforced Soil (GRS) Mass.

PLAXIS - Bentley. *Materials Model Manual*. 2020. https://communities.bentley.com/cfs-file/__key/communityserver-wikis-components-files/00-00-00-05-58/PLAXIS3DCE_2D00_V20.03_2D00_3_2D00_Material_2D00_Models.pdf.

Schlosser, Francis, and Nguyen Thanh Long. "COMPORTEMENT DE LA TERRE ARMEE DANS LES OUVRAGES DE SOUTENEMENT." *CINQUIEME CONGR. EUR. MEC. SOLS TRAV. FOND., MADRID-1972* (1972).

Schanz, T., P. A. Vermeer, and P. Gc Bonnier. "The hardening soil model: formulation and verification." *Beyond 2000 in computational geotechnics*. Routledge, 2019. 281-296.

Shukla, Sanjay Kumar, and Nagaratnam Sivakugan. "Load coefficient for ditch conduits covered with geosynthetic-reinforced granular backfill." *International Journal of Geomechanics* 13.1 (2013): 76-82.

Take, W. A., and A. J. Valsangkar. "Earth pressures on unyielding retaining walls of narrow backfill width." *Canadian Geotechnical Journal* 38.6 (2001): 1220-1230.

Terzaghi, K. (1943). Theoretical soil mechanics, John Wiley and Sons, New York, 66–76.

Thielen, D.L. and Collin, J.G., (1993). Geogrid reinforcement for surficial stability of slopes. Geosynthetics '93 Conference Proceedings, Vancouver, BC, pp. 229-244

Vulova, Christina, and Dov Leshchinsky. *Effects of geosynthetic reinforcement spacing on the behavior of mechanically stabilized earth walls*. No. FHWA-RD-03-048. United States. Federal Highway Administration. Office of Infrastructure Research and Development, 2003.

Woodruff, Ryan. *Centrifuge modeling for MSE-shoring composite walls*. Diss. University of Colorado, 2003.

Yang, Zen. *Strength and deformation characteristics of reinforced sand*. University of California, Los Angeles, 1972.

Yang Kuo-Hsin, and Liu, Chia-Nan. Finite Element Analysis of Earth Pressures for Narrow Retaining Walls. Journal of Geoengineering, Vol. 2, pp. 43-52, August 2007. http://yo-1.ct.ntust.edu.tw/jge/files/articlefiles/v2i2200709051462998162.pdf

Yang, K. H., et al. "Finite element analyses for centrifuge modeling of narrow MSE walls." *Proceedings of First Pan American Geosynthetics Conference, GEOAMERICAS*. 2008.

Yang, Kuo-Hsin, Jorge G. Zornberg, and Stephen G. Wright. *Numerical modeling of narrow MSE walls with extensible reinforcements*. No. FHWA/TX-08/0-5506-2. Texas. Dept. of Transportation. Research and Technology Implementation Office, 2008.

Yang, Kuo-Hsin, et al. "Location of failure plane and design considerations for narrow geosynthetic reinforced soil wall systems." *Journal of GeoEngineering* 6.1 (2011): 27-40.

Ziegler, M., G. Heerten, and A. Ruiken. "Progress in the understanding of geosynthetic/soil composite material behavior in geosynthetic reinforced earth structures." *1st Pan American geosynthetics conference and exhibition*. Vol. 2. No. 05. 2008.

APPENDIX

Table A.1: State of the Art Equipment

Equipment	Purpose	Results
PLAXIS 2D	The finite Element Method Program is required to simulate NMSE models with the application of secondary reinforcements	The behavior of NMSE walls with secondary reinforcements by the application of surcharge loads

BIOGRAPHICAL SKETCH

Abraham Alejandro Alvarez Reyna was raised and born in Reynosa, Tamaulipas, Mexico, on June 28th, 1994. As part of his education, he received a bachelor's degree in science of Civil Engineering in May 2017 from the University of Texas Rio Grande Valley. He was awarded the Howard Hughes Medical Institute Research (HHMI) grant in Geotechnical Engineering research during his bachelor's degree as one of the few selected in this prestigious association. Furthermore, Mr. Alvarez was actively involved in the American Society for Civil Engineers at the student chapter, where he served in several officer positions until reaching the vice-presidency. After graduating, he decided to come back to Mexico, where he began his professional experience as an Environmental Health and Safety engineer in two different manufacturing companies from 2017 to 2020.

Additionally, he received a second bachelor's degree in Civil Engineering from Universidad Mexico Americana del Norte while working in Reynosa in December 2019. Until August 2020, Mr. Alvarez began his master's degree in civil engineering, focusing on geotechnical engineering and concluded his studies in 2022. Mr. Alvarez may be reached by email at aabe.alvarez@gmail.com